Title
The in vitro characterization of heterologously expressed enzymes to inform in vivo biofuel production optimization

Author
Garcia, David Ernest

Publication Date
2013

Peer reviewed|Thesis/dissertation

The *in vitro* characterization of heterologously expressed enzymes to inform *in vivo* biofuel production optimization

By

David E. Garcia

A dissertation submitted in partial satisfaction of the

requirements for the degree of

Doctor of Philosophy

in

Chemistry

in the

Graduate Division

of the

University of California, Berkeley

Committee in charge:

Professor Jay D. Keasling, Co-chair

Professor David E. Wemmer, Co-chair

Professor Carlos J. Bustamante

Professor Adam P. Arkin

Spring 2013

ABSTRACT

The *in vitro* characterization of heterologously expressed enzymes to inform *in vivo* biofuel production optimization

by

David E. Garcia

Doctor of Philosophy in Chemistry

University of California, Berkeley

Professor Jay D. Keasling, Co-Chair

Professor David E. Wemmer, Co-Chair

The mevalonate pathway is of critical importance to cellular function as it is the conduit for the production of terpenoids, hormones, and steroids. These molecules are also valuable on an industrial scale because they are used as antibiotics, flavoring agents, and fragrances, examples of which are clerocidin, cinnamon, and sandalwood, respectively. Because the biosynthetic route for the production of these compounds is the deoxyxylulose 5-phosphate pathway in *E. coli*, by engineering the heterologous mevalonate pathway into *E. coli* the native forms of pathway regulation were overcome to successfully create a bio-industrial route for the production of artemisinin, an antimalarial drug. Advanced biofuels can also be biosynthesized via the mevalonate pathway with some minor alterations to the final enzymatic conversions. However, the toxicity of intermediates and products, as well as regulation internal to the pathway, limited our ability to increase production. The mevalonate pathway enzymes we used were native to *S. cerevisiae*, two of which had not been kinetically characterized. We set out to determine the nature of these enzymes and how they might be regulated by mechanisms internal to the mevalonate pathway, such as feedback inhibition.

Because both mevalonate kinase (MK) and phosphomevalonate kinase (PMK) were derived from *S. cerevisiae* they had to be codon-optimized for production in *E. coli*, particularly because they had already been identified as expressing poorly in laboratory production strains through targeted protein studies. By cloning the codon-optimized sequences into high copy expression vectors with a six-histidine tag at the C- or N-terminus (PMK and MK, respectively) we were able to produce large enough amounts of the active proteins to purify on a Ni^{2+} resin column.

Kinetic characterization of MK revealed a K_M^{ATP} of 315 ± 21 µM and a v_{max} of 50 ± 3 µM/min/µgE (or K_{cat} = 41 ± 3 s^{-1}). Additionally, substrate inhibition of MK by mevalonate was determined to exist at concentrations above 2.5 mM, and K_i values for farnesyl pyrophosphate (79 ± 11 nM), geranyl pyrophosphate (147 ± 6 nM), geranylgeranyl pyrophosphate (303 ± 64 nM), dimethylallyl pyrophosphate, (29 ± 12 µM), and isopentenyl pyrophosphate (36 ± 5 µM) were determined.

Kinetic characterization of PMK revealed that maximum activity occurs at pH = 7.2 and [Mg^{2+}] = 10 mM. K_M^{ATP} was determined to be 98.3 µM and 74.3 µM at 30 °C and 37 °C, respectively. $K_M^{mev\text{-}p}$ was determined to be 885 µM and 880 µM at 30 °C and 37 °C, respectively. v_{max} was determined to be 45.1 µmol/min/µgE and 53.3 µmol/min/µgE at 30 °C and 37 °C, respectively. From the high $K_M^{mev\text{-}p}$ value it appears as if PMK might have very poor activity at normal cellular concentrations of mevalonate-5-phosphate, indicating that MK and PMK might play a very coordinated role in balancing intermediate levels within the pathway.

Table of Contents

Acknowledgements

Jay, you are a first-class advisor (given that you are my third advisor in graduate school I have enough data to assure you that me saying so is not just a platitude). You took me in when no one else would have me, gave me the time to learn an entirely new field of science, graciously allowed me to explore outside interests (both personal and professional), and were so empathic and accommodating when my personal and professional spheres exploded in a fiery collision (I think we both know what I'm referring to here) that I don't think I could have ask for a better guiding hand through graduate school. You are amazing.

Mom and Dad, I doubt you'll ever read this, but I appreciate the unconditional support and love you give, which made the wealth of hard times so much more bearable.

Rita and Kat, I also doubt you'll ever read this, but one of the two of you has always been there for me regarding the stuff one can't talk about with the parental units. Thanks for that. Also, I would like to thank Rita for reminding me to thank grant number TWO FOUR SIX OH OOOONE.

Achilles and Patroclus, I miss you two like crazy. Circumstances outside of our control are ultimately responsible for your being with me less time than we ought to have had together, but I still feel guilty nonetheless. I take solace in the fact that you two live on as very minor YouTube sensations.

Alcohol, you got me through undergrad and grad school, and I'm sure you'll be there for me for the rest of my life. You are truly my best friend. Cheers!

That special someone who isn't yet in my life, I'm sorry we weren't dating/engaged/married by the time I wrote this because it would be really cool to acknowledge you here. I asked, but they won't let me change this after I submit it so you'll just have to trust me when I say that this paragraph was always meant for you, _____.

Chapter 1. Introduction and motivation

1.1 Introduction

I joined the Keasling lab after having spent three years in graduate school researching the dissociation pathways of non-specific, non-covalent, gas-phase clusters of proteins and peptides. This work, and my undergraduate studies, did not prepare me for the research I would eventually perform in the Keasling lab. Although the Keasling lab has always had the analytical-chemistry wherewithal to get the information necessary to be successful in its research endeavors, at that time the lab was just ramping up its analytical capabilities to expand into proteomics and metabolomics. Both of these profiling methods rely entirely on mass spectrometry, an analytical technique that I was more than familiar with because my first research project was performed entirely inside a Fourier Transform Ion Cyclotron Resonance Mass Spectrometer. Given my "expertise" it seemed natural that my first role in the lab was to help other people with their analytical chemistry while I essentially went back to undergrad to learn the basics of biology.

While I was tackling simple things like growth curves and sterile technique, the excitement over the data generated from proteomic and metabolic profiles was palpable. These techniques were greatly expanding our ability to assess the phenotypic differences in the strains the lab was engineering. This information is undeniably valuable, but even early on it became clear that sometimes these large profiling techniques generated as many questions as they answered. For example, why are two proteins that should be expressed at similar levels not? One direction research expanded to address this question was transcriptomics and fluxomics. Together with genomics these techniques round out the so-called *'omics* techniques. Rather than go large, however, my training had imbued me with a careful set of hands and the desire to drill down on something specific. Fortunately, just such a project opened up in the lab at the time we transitioned from engineering artemisinin/amorphadiene (an anti-malarial drug and one of its chemical precursors) producing strains of *E. coli* and *S. cerevisiae* to biofuel producing strains. This project was the kinetic characterization of two enzymes that had been identified as potentially limiting our ability to increase biofuel production titers.

Taking a step back, under normal circumstances one should find that the velocity of an enzyme-catalyzed reaction obeys the Michaelis-Menten equation (Equation 1). The details of this equation are covered in depth in any basic biochemistry textbook, so here we will simply summarize this equation as relating the velocity of the reaction (what we can observe in lab) to the maximum speed of the reaction (v_{max}) and the concentration of substrate necessary to achieve half of v_{max} (K_M). It is important to note that when an enzyme acts on more than one

substrate, one enzyme must be held in saturating conditions in order for the equation to accurately describe the K_M of the other substrate.

$$v = \frac{v_{max} * [S]}{K_M + [S]}$$

Equation 1. The Michaelis-Menten equation.

In a vacuum, traditional enzyme kinetics can seem like a bit of a futile exercise because, to inappropriately misquote Shakespeare, "what's in a v_{max}?" Unless you are at the extreme ends of the spectrum a number in isolation doesn't mean much. However, since the ultimate goal of the Keasling lab is to turn microorganisms into miniature chemical factories, knowing these two values can help us choose which exogenous enzymes to incorporate into our production strains when more than one option exists. One might be tempted to think that simply finding enzymes with the fastest v_{max} and lowest K_M would be the name of the game, and in a one step conversion *in vitro* it might be. However, when one considers the more complicated picture of metabolic pathways *in vivo*, enzyme regulation becomes a very important consideration. Because we are engineering a heterologous metabolic pathway it is less likely that there will be much native regulation to engineer around. However, downstream metabolic intermediates that are toxic to the cell at high concentrations may have favored the evolution of feedback inhibition on an upstream enzyme; this mechanism of limiting flux through a pathway will "come along for the ride" even if the enzymes are expressed heterologously.

In order to figure out how to engineer around feedback inhibition one needs to know whether it is competitive or noncompetitive inhibition. The two types are easy to distinguish in the lab because competitive inhibitors cause the apparent K_M to increase while v_{max} remains the same, while noncompetitive inhibition does not alter K_M, but does lower v_{max} (Figure 1). In the case of competitive inhibition, as the name suggests one must have a higher concentration of substrate in order to outcompete the inhibitor for presence in the binding site and achieve maximal reaction velocity. This might be accomplished by altering protein expression levels to control intermediate concentrations. Noncompetitive inhibition lowers the effective enzyme concentration by inactivating enzymes. This can only be reasonably overcome in our system by reengineering the enzyme to bind its inhibitor less strongly because increasing enzyme concentration will only decrease the theoretical production limit of biofuel. Of course, if the inhibitor binding is reversible then another option would be to find an enzyme that rids the system of the inhibitor as quickly as possible.

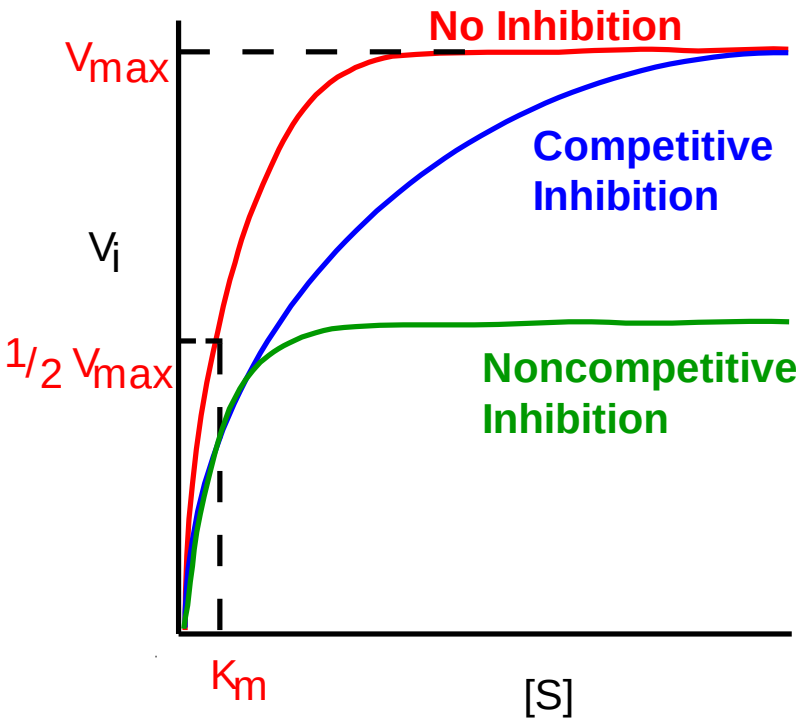

Figure 1. Graphic representation of how competitive and noncompetitive inhibition affects K_M and v_{max}.

1.2 Motivation

The Mevalonate Pathway

In *S. cerevisiae* the mevalonate pathway is the conduit for producing isopentenyl pyrophosphate (IPP) and dimethylallyl pyrophosphate (DMAPP), which are then converted into the terpenoids (Wilding, *et al.*, 2000, Kuzuyama, 2002), hormones and steroids (Kuzuyama & Seto, 2012) crucial to survival; *E. coli* accomplishes the synthesis of IPP and DMAPP through the deoxyxylulose 5-phosphate pathway (DXP) (Bochar, *et al.*, 1999, Wilding, *et al.*, 2000, Kuzuyama, 2002, Hedl, *et al.*, 2004). By engineering the mevalonate pathway into *E. coli* the Keasling lab has been able to increase production of sesquiterpenes, such as the antimalarial drug artemisinin, by bypassing the regulatory mechanisms of the native DXP pathway (Martin, *et al.*, 2003, Ro, *et al.*, 2006, Chang, *et al.*, 2007).

The chemical structures of the intermediates in the mevalonate pathway and the molecules they turn into (Figure 2) make them interesting targets for biofuels (Bokinsky, *et al.*, 2011, Peralta-Yahya, *et al.*, 2011). As phosphorylated and pyrophosphorylated compounds these intermediates do not make good biofuels, but simple modifications can be made either *in vivo* or through traditional chemical engineering processes post cellular culture extraction that would transform them into biofuels that could offset or replace traditional liquid fuels (Zhang, *et al.*, 2011). Although corn-based ethanol is already a reality in the energy market, ethanol is a less than desirable biofuel because not only does it divert crops from the food supply, it is not compatible with our current distribution infrastructure or vehicle fleet (Lee, *et al.*, 2008), whereas the fuels we can make from the mevalonate pathway are *advanced biofuels* that would be compatible with our current distribution infrastructure and vehicle fleet.

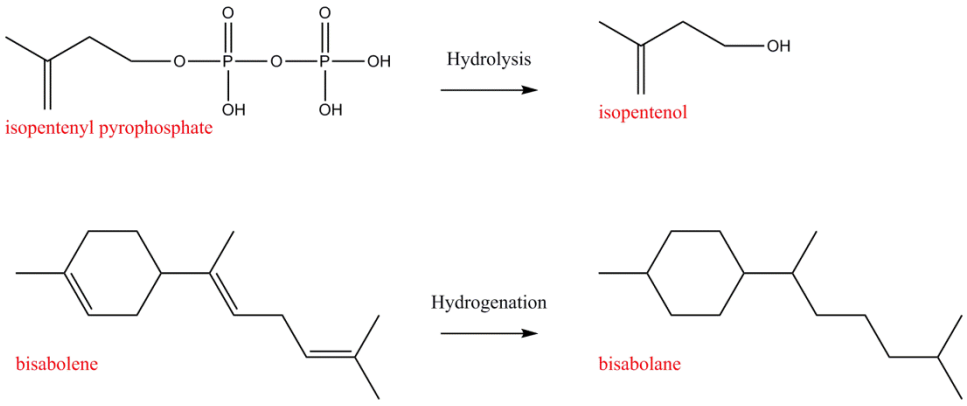

Figure 2. A mevalonate pathway intermediate (IPP) and a downstream metabolite (bisabolene) and how they might be altered, *in vivo* or *in vitro*, to be suitable biofuels.

Mevalonate Kinase

MK catalyzes the conversion of mevalonate and ATP to mevalonate-5-phosphate and ADP (Figure 3). Most known MKs are feedback inhibited to some degree and a structural basis is being elucidated to explain why some MKs are more inhibited by prenyl phosphates than others (Fu, *et al.*, 2008, Primak, *et al.*, 2011). From this work it seems most likely that the pyrophosphate end of prenyl phosphates binds to the same site as the triphosphate region of ATP. The assumption that *S. cerevisiae* MK is feedback inhibited is, therefore, reasonable. Determining whether the MK we have engineered into our production strains is a good choice can only be accomplished by determining its kinetic constants and what, if any, intermediates inhibit its activity. This is made even more important by proteomics data that has previously shown MK is expressed at relatively low levels and may be a target for increasing overall fuel production (Redding-Johanson, *et al.*, 2011, Singh, *et al.*, 2012).

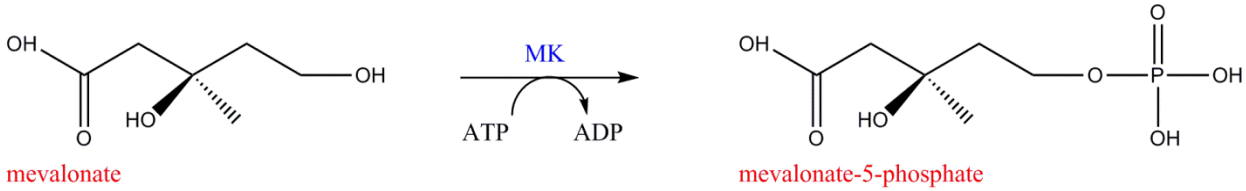

Figure 3. Mevalonate and ATP are converted to mevalonate-5-phosphate and ADP by MK.

Phosphomevalonate Kinase

PMK is a phosphotransferase that acts on mevalonate-5-phosphate and ATP to yield mevalonate-5-diphosphate (Figure 4). Because PMK has a similar mode of activity as MK, downstream prenyl phosphates might act as general ATP binding site inhibitors on PMK as well, making it another potential source of mevalonate pathway regulation.

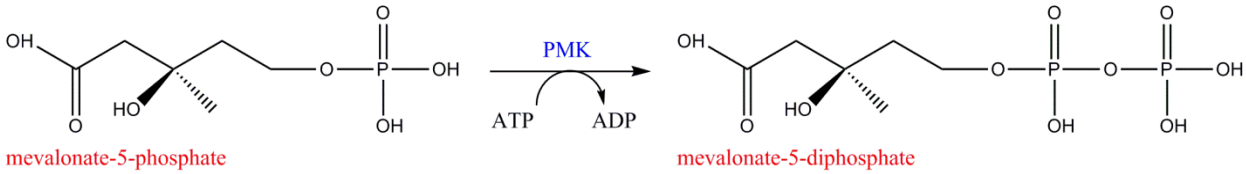

Figure 4. Mevalonate-5-phopsphate and ATP are converted to mevalonate-5-diphosphate and ADP by PMK.

PMK also has the potential to be a problematic enzyme for biofuel production because other sources of PMK have been shown to be Mn^{2+} dependent rather than Mg^{2+} dependent (Doun, *et al.*, 2005) and substrate inhibited by ATP under high ATP, low mevalonate-5-phosphate concentrations (Eyzaguirre, *et al.*, 2006). A full characterization of PMK could reveal interesting regulation or cofactor requirements.

Chapter 2. The effect substrate inhibition on Mevalonate kinase from *Saccharomyces cerevisiae* has on 3-hydroxy-3-methyl-glytaryl-coenzyme A reductase[1]

2.1 Introduction

Microbial production of desirable compounds through heterologous expression of foreign pathways commonly results in unintended consequences. Introduction of previously unknown and potentially toxic metabolites in the host organism may result in lower cell density and reduced product formation. Maintenance of a delicate balance between utilization of existing cellular resources for organism growth versus engineered manipulations such as enzyme overexpression is therefore an important aspect of metabolic optimization. Consequently, metabolic engineering strategies reported thus far have investigated accumulation of toxic intermediates (Berry*, et al.*, 2002, Zhu*, et al.*, 2002, Pitera*, et al.*, 2007), targeted improvements in protein production (Glick, 1995, Redding-Johanson, *et al.*, 2011), kinetics of rate limiting processes (Pfleger *et al.*, 2006), spatial localization of key enzymatic activities (Pfleger, *et al.*, 2006, Zhang, *et al.*, 2008, Dueber, *et al.*, 2009, Chhabra & Keasling, 2011), and redox cofactor utilization by pathway components (Berrios-Rivera, *et al.*, 2002, San, *et al.*, 2002, Bennett & San, 2009).

The isoprenoid biosynthetic pathway is an important source of biopharmaceuticals, biochemicals, and advanced biofuels (Fortman, *et al.*, 2008). In nature, terpenoids are synthesized from the universal precursors (isopentenyl pyrophosphate (IPP) and its isomer dimethylallyl pyrophosphate (DMAPP), which are generated either through the mevalonate (MEV) pathway or the deoxyxylulose 5-phosphate (DXP) pathway (Bochar, *et al.*, 1999, Wilding, *et al.*, 2000, Kuzuyama, 2002, Hedl, *et al.*, 2004). Generally, Gram-negative bacteria and eukaryotic organelles employ the DXP pathway, while humans, mammals, other eukaryotes, archaea and gram-positive cocci utilize the enzymes and intermediates of the mevalonate pathway (Bochar, *et al.*, 1999, Hedl, *et al.*, 2004). In *Escherichia coli* and other gram-negative bacteria, IPP and DMAPP generated from the natively regulated DXP pathway are essential metabolites for the prenylation of tRNAs and the synthesis of farnesyl pyrophosphate, which is central for quinine and cell wall biosynthesis (Connolly & Winkler, 1989). Enhanced sesquiterpene production in *E. coli* has been accomplished through the heterologous

1 Partially reproduced with permission from Ma SM, Garcia DE, Redding-Johanson AM, *et al*. (2011) Optimization of a heterologous mevalonate pathway through the use of variant HMG-CoA reductases. Metabolic Engineering 13: 588-597. Copyright 2011 Metabolic Engineering.

expression of the MEV pathway from *Saccharomyces cerevisiae* thereby bypassing the regulatory effects of its native DXP pathway (Martin*, et al.*, 2003, Pitera*, et al.*, 2007, Harada & Misawa, 2009). While this foreign MEV pathway is potentially unregulated in *E. coli*, its presence affects cellular behavior in significant ways. Notably, accumulation of the pathway intermediate 3-hydroxy-3-methyl-glutaryl-coenzyme A (HMG-CoA) has been shown to lead to bacterialstatic and bactericidal effects (Pitera*, et al.*, 2007). In addition, enzymatic conversion of HMG-CoA into mevalonate is the only redox cofactor utilization step in the entire MEV pathway and has the potential to disturb cellular redox balance (Berrios-Rivera*, et al.*, 2002, Heuser*, et al.*, 2007). The catalytic reaction performed at the HMG-CoA reductase step therefore represents a crucial bottleneck where metabolic engineering strategies may be applied to optimize the system for isoprenoid biosynthesis.

HMG-CoA reductase (HMGR), one of the few known four-electron oxidoreductases in nature, catalyzes the reduction of (S)-HMG-CoA to (R)-mevalonate (Figure 5). Two moles of reduced pyridine nucleotide coenzyme are oxidized during the reduction of 1 mole of the thioester group of HMG-CoA to the primary hydroxyl group of mevalonate. HMGR is also able to catalyze the reverse reaction, the oxidative acylation of (R)-mevalonate to (S)-HMG-CoA. Based on sequence divergence, two classes of HMGRs have been proposed (Bischoff & Rodwell, 1992, Rodwell*, et al.*, 2000, Boucher*, et al.*, 2001, Istvan, 2001). Conventionally, class I HMGRs are typically found in higher organisms, generally prefer NADPH as the cofactor (Lawrence, *et al.*, 1995), and under physiological conditions, are effectively irreversible even though isolated enzymes catalyze the reaction in both direction (Sherban, *et al.*, 1985, Bach, *et al.*, 1986, Lawrence, *et al.*, 1995). In contrast, class II HMGRs comprise those from prokaryotes and archaea and generally prefer NADH as a cofactor (Kim, *et al.*, 2000, Theivagt, *et al.*, 2006).

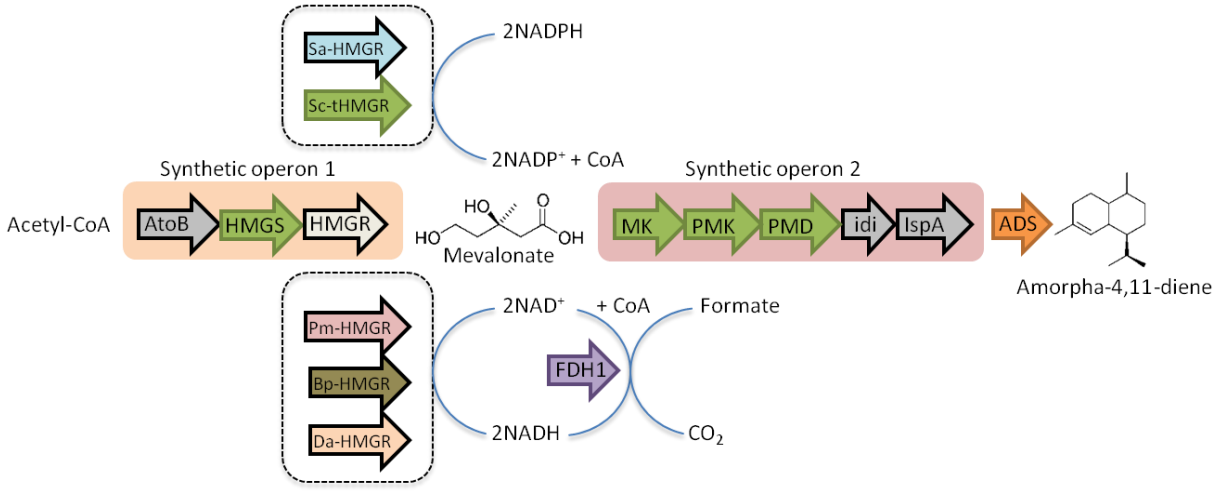

Figure 5. Biosynthetic mevalonate pathway for isoprenoid production in *E. coli* towards amorpha-4,11-diene synthesis.

It is well known that pathway optimization is a complex interplay of factors such as: toxicity associated with newly introduced metabolites, disturbance in cellular redox state, *in vivo* enzymatic activity, and suboptimal protein expression levels. Previous efforts to alleviate the bottleneck at HMG-CoA reductase catalysis in microbial isoprenoid biosynthesis focused on manipulating features of only the native HMGR of the *S. cerevisiae* MEV pathway. These included modulation of enzyme production (Pitera*, et al.*, 2007), regulated enzyme production (Pfleger, *et al.*, 2006), and post-translational localization (Zhang, *et al.*, 2008). The overall goal of this study was to alleviate the bottleneck associated with the HMG-CoA reduction step by perturbing enzymatic properties of HMGR while maintaining existing features of the engineered MEV pathway intact. Herein we report our efforts to examine how mevalonate kinase (MK), the enzyme immediately downstream from HMGR, influences the desirable kinetic properties of the ideal HMGR.

2.2 Results and Discussion

We measured the initial reaction rates of the *S. cerevisiae* mevalonate kinase under ATP saturating conditions with increasing levels of mevalonate and found that the fastest average reaction rate was observed around 2.5 mM mevalonate (Figure 6). At mevalonate concentrations greater than this concentration the reaction rate of the *S. cerevisiae* MK begins to decrease. Substrate inhibition at high mevalonate concentrations has also been reported previously for the MK from *S. aureus* (Voynova, *et al.*, 2004). This suggests that HMGRs with very high forward reaction rates could have detrimental effects on production levels of the final product amorphadiene due to substrate inhibition at the pathway step mediated by MK catalysis. This also opens up the intriguing possibility of improving production levels through appropriate protein engineering of MK to complement previous efforts in improving MK expression levels (Anthony, *et al.*, 2009, Redding-Johanson, *et al.*, 2011). A potential mechanism for substrate inhibition could include a competitive binding inside the active site, as was suggested recently for ferrochelatase (Hunter & Ferreira, 2010). Upon mutation of a single residue near the binding pocket of this enzyme, substrate inhibition was lowered by two orders of magnitude, and a mutation directly inside the binding site eliminated substrate inhibition entirely. This mutation in the binding pocket, while eliminating substrate inhibition, also resulted in disruption of the complex substrate-enzyme interaction resulting in a dramatically reduced ability of ferrochelatase to catalyze at low substrate concentrations, displaying the intricacy of this protein engineering challenge. A similar approach to mutate the allosteric mevalonate binding site of MK could potentially be employed to improve the kinetic behavior of this enzyme. The vital component is to eliminate or shift the threshold MK substrate inhibition point while maintaining its ability to catalyze at low mevalonate concentrations. In conclusion, we postulate that superior performance of the *D. acidovorans* HMGR for amorphadiene production may be attributed to its kinetic ability to fine tune the balance between HMG-CoA levels below the cellular toxicity threshold and the mevalonate levels below concentrations that inhibit MK activity.

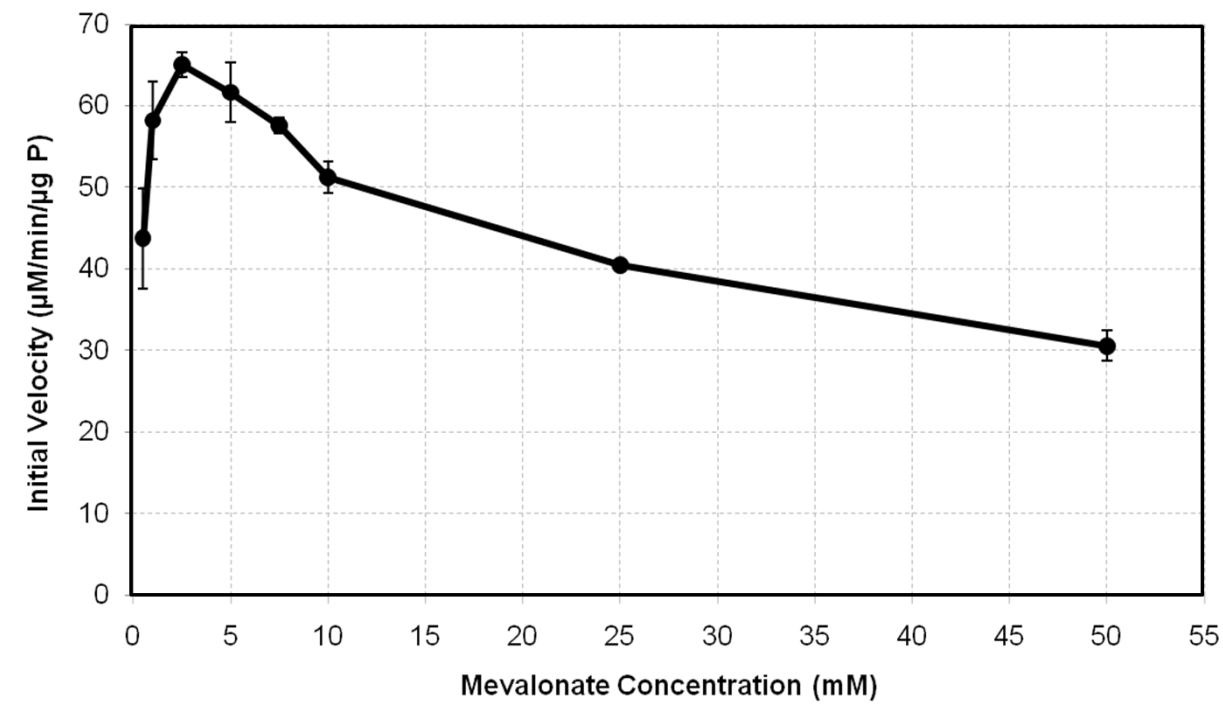

Figure 6. Substrate inhibition of *S. cerevisiae* mevalonate kinase by mevalonate.

2.3 Methods and Materials

Activity Assay

All chemicals and enzymes were purchased from Sigma-Aldrich. *S. cerevisiae* mevalonate kinase (MK), was a gift from Amyris Biotechnologies (Emeryville, CA). All non-enzyme solutions were 0.2 µM filter-sterilized (P.N. 190-2520, Thermo Scientific). β-Nicotinamide adenine dinucleotide (NADH), phosphoenolpyruvate (PEP), mevalonate, and ATP (adjusted to pH = 7.0, filter-sterilized in 2.0 M tris-base), were kept frozen (-20 °C). The extinction coefficients of ATP (15.4 $mM^{-1}cm^{-1}$ at 259 nm) and NADH (6.22 $mM^{-1}cm^{-1}$ at 339 nm) were used to determine stock concentrations. Mevalonate was made by the saponification of mevalonolactone with KOH at 1.5:1 (mol:mol) KOH:mevalonolactone for 2 hours at 37 °C, 200 rpm. Conversion was verified via normal phase TLC developed in isopropanol and stained with basic permanganate, and titrated to pH = 7.0. 1 mL enzymatic assay mixtures contained: 200 mM Tris-HCl (pH = 7.0), 100 mM KCl, 6 mM $MgCl_2$, 0.24 mM NADH, 3.0 mM ATP, 1.0 mM PEP, 0.5-50 mM mevalonate, 6.82 U pyruvate kinase, 9.90 U lactate dehydrogenase, and 1 µg MK. Reactions progress at 30 °C and were monitored spectrophotometrically at 339 nm for NADH consumption. Triplicate reactions were performed for statistical analysis, from which average reaction velocities were calculated in µM product formed per minute per µg MK added. To ensure MK was the rate-limiting enzyme, when necessary the following standard controls and results were verified: doubling the MK added doubled the observed rate, doubling the supporting enzymes added did not affect the observed rate, and doubling the phosphoenolpyruvate concentration did not affect the observed rate.

Chapter 3. The expression, purification, and kinetic characterization of Mevalonate kinase from *Saccharomyces cerevisiae* and *Methanosarcina mazei*

3.1 Introduction

It had been "common knowledge" in the Keasling lab that *S. cerevisiae* mevalonate kinase (MK) is inhibited by farnesyl pyrophosphate despite the fact that experiments had never been done to confirm this notion. The hallmark of competitive inhibition is an accumulation of substrate and the accumulation of mevalonate had been noted in previous work done in the lab (Martin, *et al.*, 2003, Pfleger, *et al.*, 2006). Given that MKs from other sources are well known to be feedback inhibited—for which a structural basis is being elucidated (Fu, *et al.*, 2008, Primak, *et al.*, 2011)—the assumption that *S. cerevisiae* MK is feedback inhibited is reasonable; however, it is not the only explanation for the phenomenon. The classic method for overcoming competitive feedback inhibition is to drive up substrate concentration, but in doing so the mevalonate concentrations measured in production strains ended up so high that MK moved into its previously unknown substrate inhibition regime. This substrate inhibition of MK is why the best production titers came from a strain of *E. coli* harboring a heterologous metabolic pathway engineered to produce amorphadiene that contained a reversible 3-hydroxy-3-methyl-glytaryl-coenzyme A reductase (the enzyme responsible for converting 3-hydroxy-3-methyl-glytaryl-coenzyme A into mevalonate) (Ma, *et al.*, 2011). Thus, the observation of a metabolic bottleneck at MK via the accumulation of mevalonate may be due solely to substrate inhibition, or it may be that it MK is also inhibited by downstream metabolites and can only function efficiently in a narrow window of conditions. If one were to toss caution and charity to the wind one could say that if the latter is true then MK is "designed" not to work. This made the complete characterization of MK all the more vital so that we could be certain which downstream metabolites, if any, are inhibitors of MK and to what degree they affect MK activity because this will directly affect our ability to increase biofuel production. Because we have focused on the use of the mevalonate pathway the array of fuel targets being pursued by research in the Keasling lab are prenyl and terpene based. This implicates isopentenyl pyrophosphate (IPP), dimethylallyl pyrophosphate (DMAPP), geranyl pyrophosphate (GPP), farnesyl pyrophosphate (FPP), and geranylgeranyl pyrophosphate (GGPP) as the most important possible inhibitors (Figure 7).

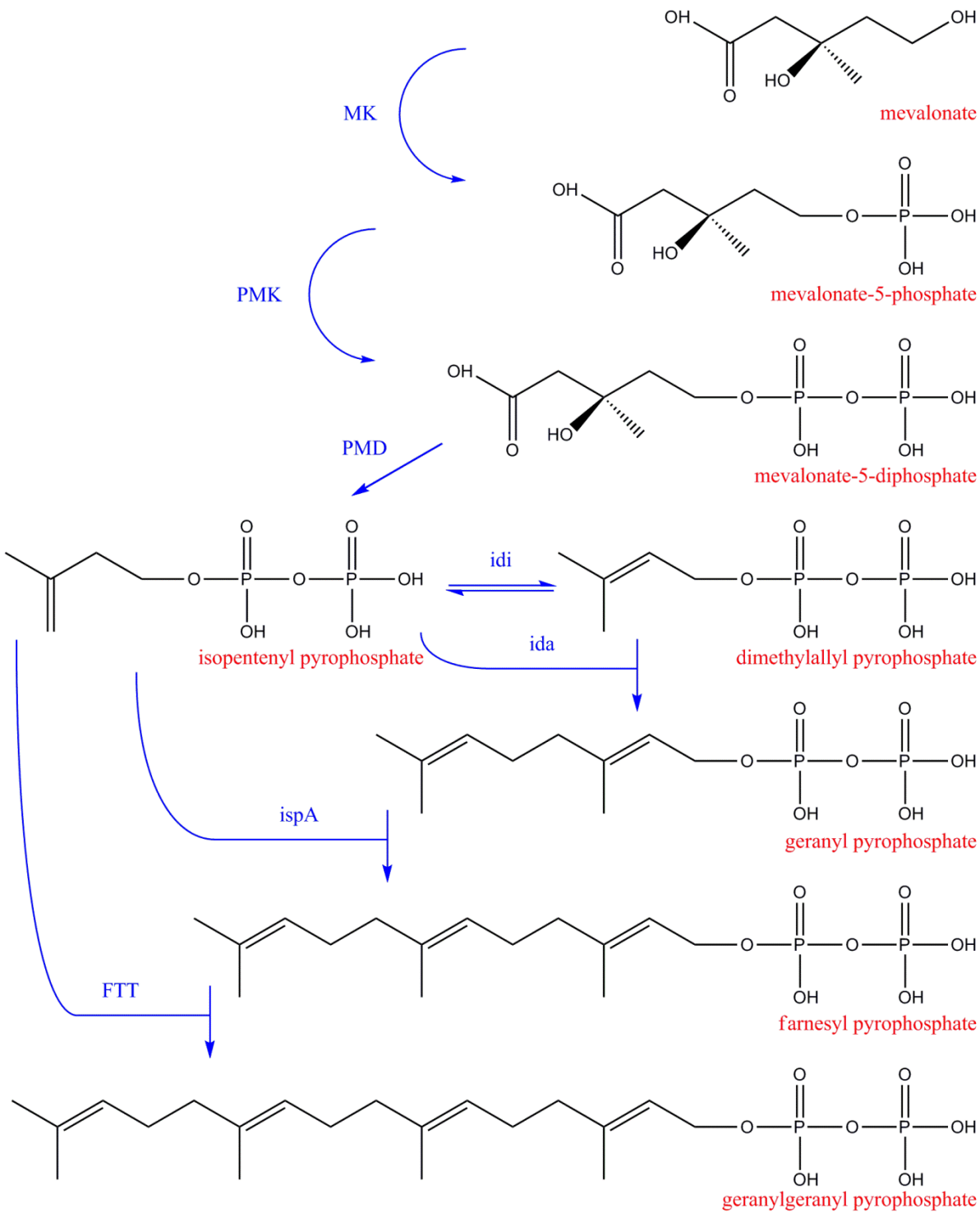

Figure 7. The portion of the mevalonate pathway downstream from MK from which the inhibitors tested were selected. Mevalonate kinase (MK), phosphomevalonate kinase (PMK), phosphomevalonate decarboxylase (PMD), Isopentenyl pyrophosphate isomerase (idi), Dimethyallylpyrophosphate transferase (ida), Farnesyl pyrophosphate synthase (ispA), Farnesyltranstransferase (FTT).

Mevalonate-5-phosphate (mev-p) and mevalonate-5-diphosphate (mev-pp) are also possible inhibitors, but neither could be studied because they were not commercially available at the time of these experiments. Because we are using a coupled assay that allows the near continuous monitoring of reaction progress over a long time frame; by keeping the initial substrate concentration constant we can discover if mev-p is an inhibitor of MK because the reaction velocity will decrease as more mev-p is produced (Figure 8). One method to deal with this possibility would be the addition of purified, active phosphomevalonate kinase (PMK) to rid the reaction mixture of any mev-p produced. However, this approach has a drawback in that it just converts one inhibitor (mev-p) into another potential inhibitor (mev-pp). The most experimentally feasible way to deal with this challenge should it arise is to monitor reaction progress until the velocities measured are no longer linear and to remove that data from the initial velocity fit. This would limit the advantage of lengthy initial velocity measurement inherent in this coupled assay, but the other advantages—easy spectrophotometric monitoring, no need to sample or take time points, eliminate potential ADP inhibition—continue to make it the best method for conducting this experiment. It should be noted that when ATP is not the limiting substrate this coupled assay does not allow lengthy initial velocity measurement because it does not regenerate mevalonate; in this case linearity of the initial reaction velocity data must be selected manually, so doing the same if mev-p turns out to inhibit MK activity is essentially trivial.

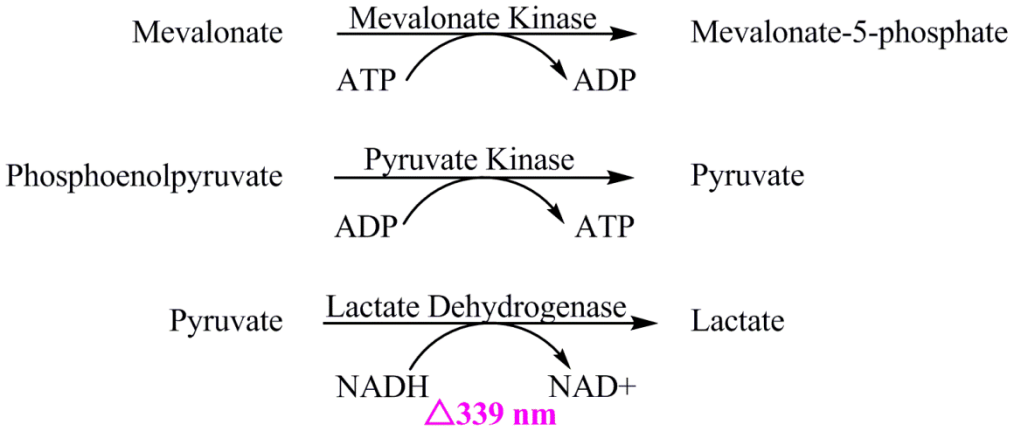

Figure 8. A spectrophotometric coupled assay that allows for the determination of kinetic constants if the ATPase, in this case mevalonate kinase, is the rate-limiting step.

3.2 Discussion and Results

When these experiments were started MK from *S. cerevisiae* had not been characterized. As is sometimes the case in science, because this information is so important, another group published a full characterization of *S. cerevisiae* MK (Primak, *et al.*, 2011) while we were midway through our studies. While this was a barrier to publishing these results in a peer-reviewed journal, it does not preclude inclusion in a dissertation. The silver-lining of having been "scooped" is that we are able to compare our results to the published characterization, which align very closely.

The K_M^{ATP} of MK was 315 ± 21 µM and the v_{max} was 50 ± 3 µM/min/µgE (or k_{cat} = 41 ± 3 s^{-1}). Although this fairly high value for K_M^{ATP} might call into question whether the enzyme is at all functional under normal physiological conditions for typical metabolites that persist at lower concentrations, ATP concentration *in vivo* is higher than the reported K_M (Schneider & Gourse, 2004, von Ballmoos, *et al.*, 2009). An enzyme whose function isn't critical to normal cellular operations should not tax energy reserves, warranting a higher K_M; however, in order for the enzyme to function effectively in that circumstance the k_{cat} should be fairly fast so that substrate can be converted to product before it dissociates from of the binding pocket.

MKs derived from most sources are competitively inhibited by mevalonate pathway intermediates, including human (Hinson, *et al.*, 1997, Potter, *et al.*, 1997), pig (Dorsey & Porter, 1968), and a variety of other microorganisms (Andreassi, *et al.*, 2004, Voynova, *et al.*, 2004, Andreassi, *et al.*, 2007, Fu, *et al.*, 2008). *S. cerevisiae* MK is also strongly competitively inhibited by downstream mevalonate pathway intermediates as summarized in Table 1 below. Although mevalonate phosphate was not tested as an inhibitor on its own, when no inhibitors were added there was no diminishment of the reaction velocity over the 15-20 minute observation window, indicating mevalonate phosphate does not inhibit MK.

Table 1. Summary of mevalonate kinase inhibition results.

Inhibitor	K_i
Farnesyl pyrophosphate	79 ± 11 nM
Geranyl pyrophosphate	147 ± 6 nM
Geranylgeranyl pyrophosphate	303 ± 64 nM
Dimethylallyl pyrophosphate	29 ± 12 µM
Isopentenyl pyrophosphate	36 ± 5 µM

The classification of inhibition as competitive (having the same v_{max}, but different K_M) is clear in regression analysis of the data for all inhibitors tested. FPP was the strongest inhibitor tested

(Figure 9 and Figure 10), followed by GPP (Figure 11 and Figure 12), GGPP (Figure 13 and Figure 14), DMAPP (Figure 15 and Figure 16), and then IPP (Figure 17 and Figure 18).

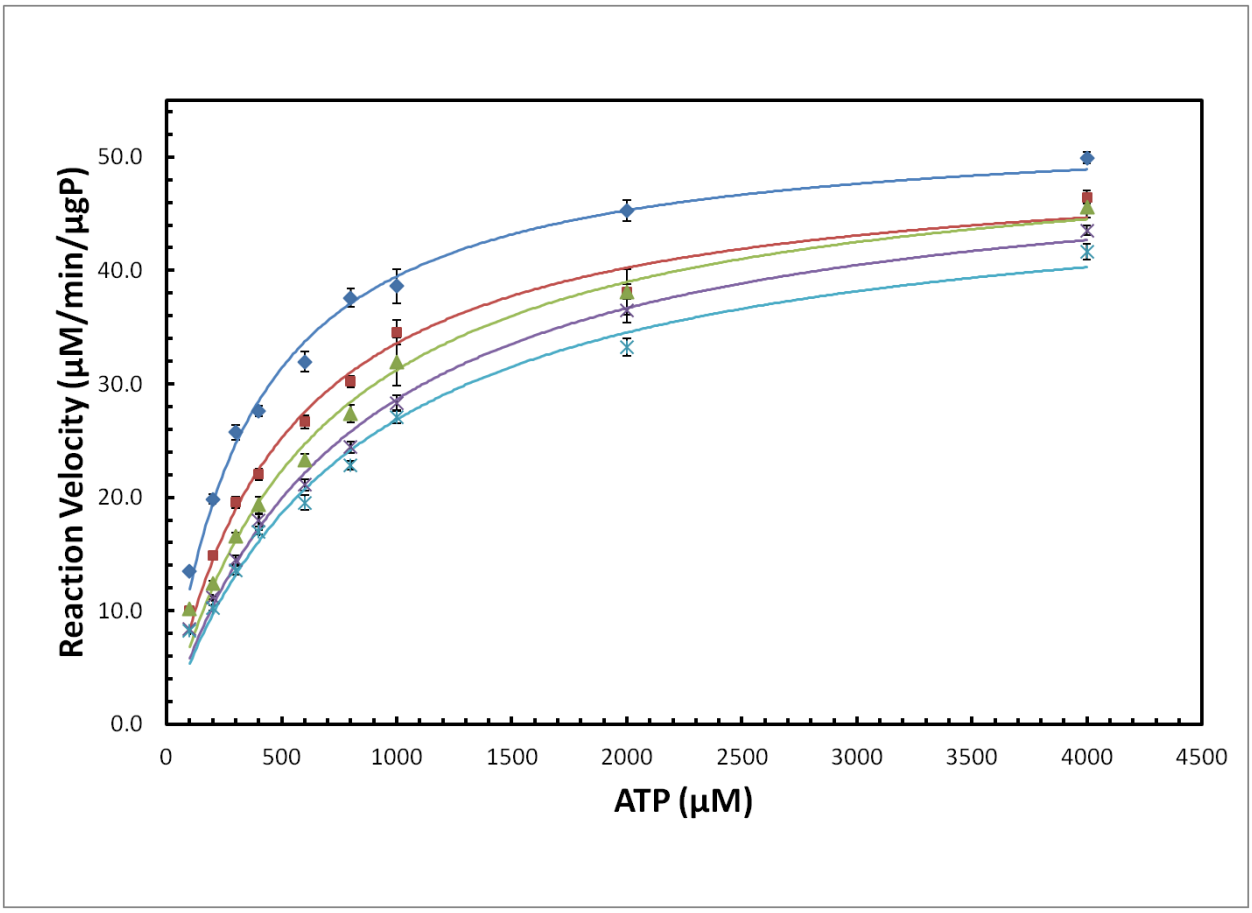

Figure 9. Competitive inhibition of mevalonate kinase by farnesyl pyrophosphate at 0 nM (dark blue), 25 nM (red), 50 nM (green), 75 nM (purple), and 100 nM (light blue).

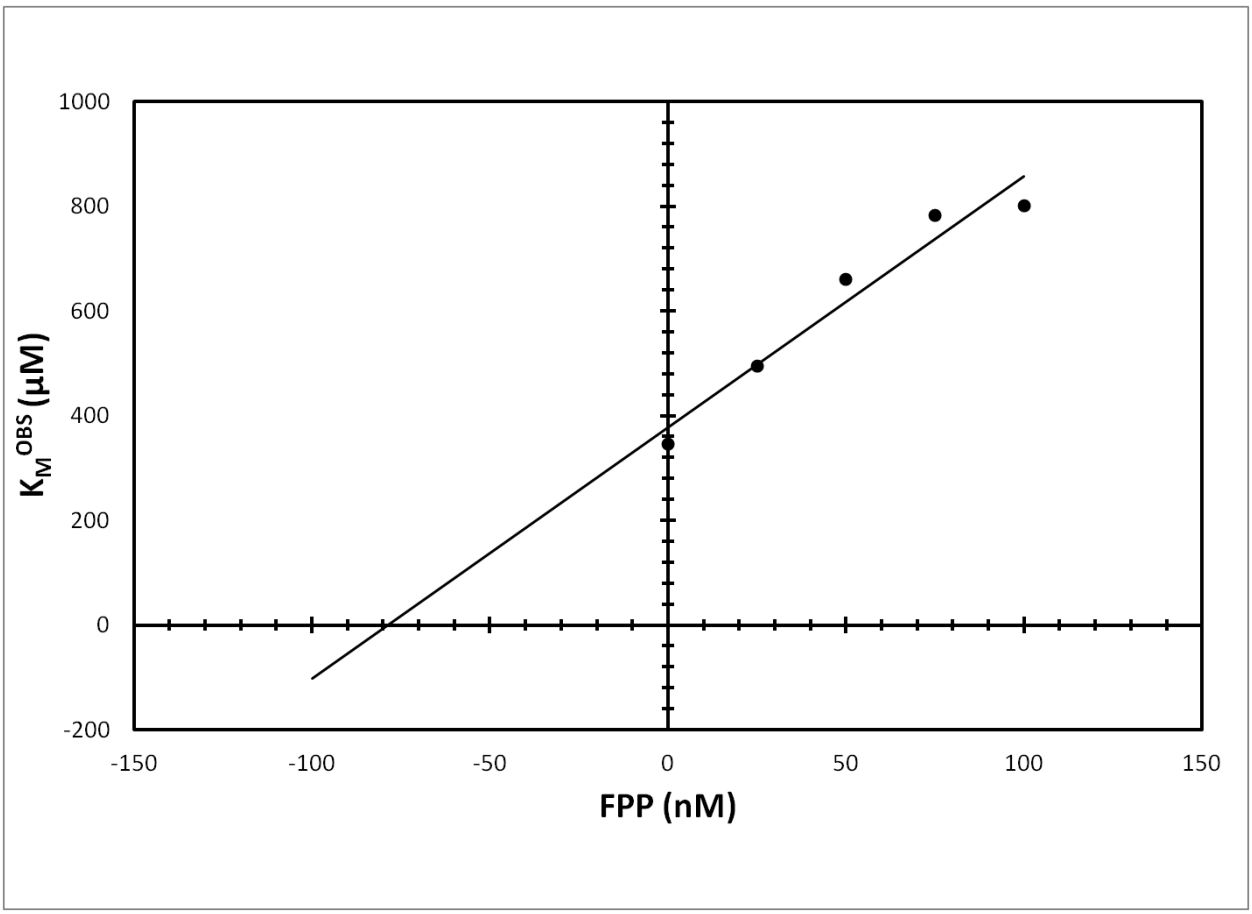

Figure 10. The K_i for farnesyl pyrophosphate on mevalonate kinase is 79 ± 11 nM.

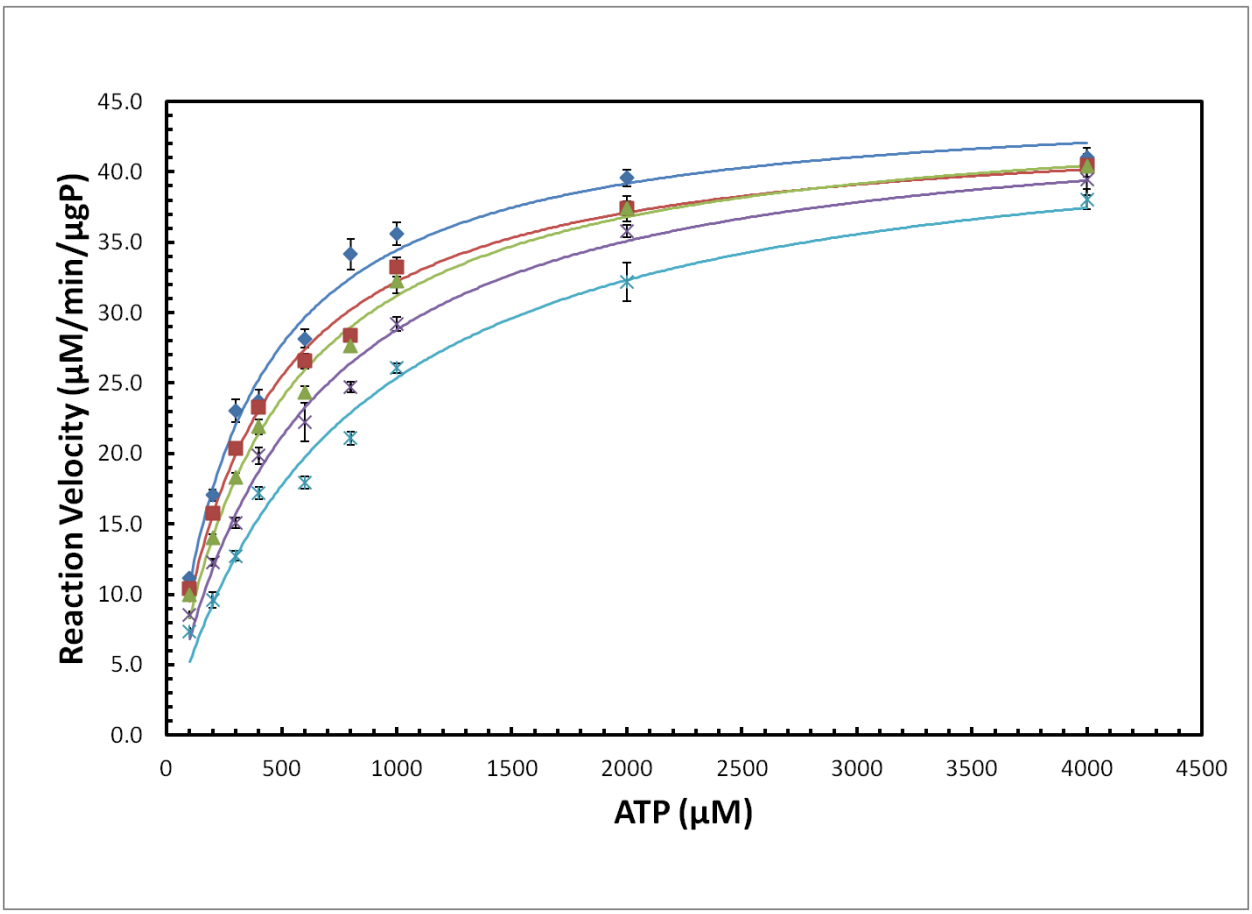

Figure 11. Competitive inhibition of mevalonate kinase by geranyl pyrophosphate at 0 nM (dark blue), 20 nM (red), 50 nM (green), 100 nM (purple), and 200 nM (light blue).

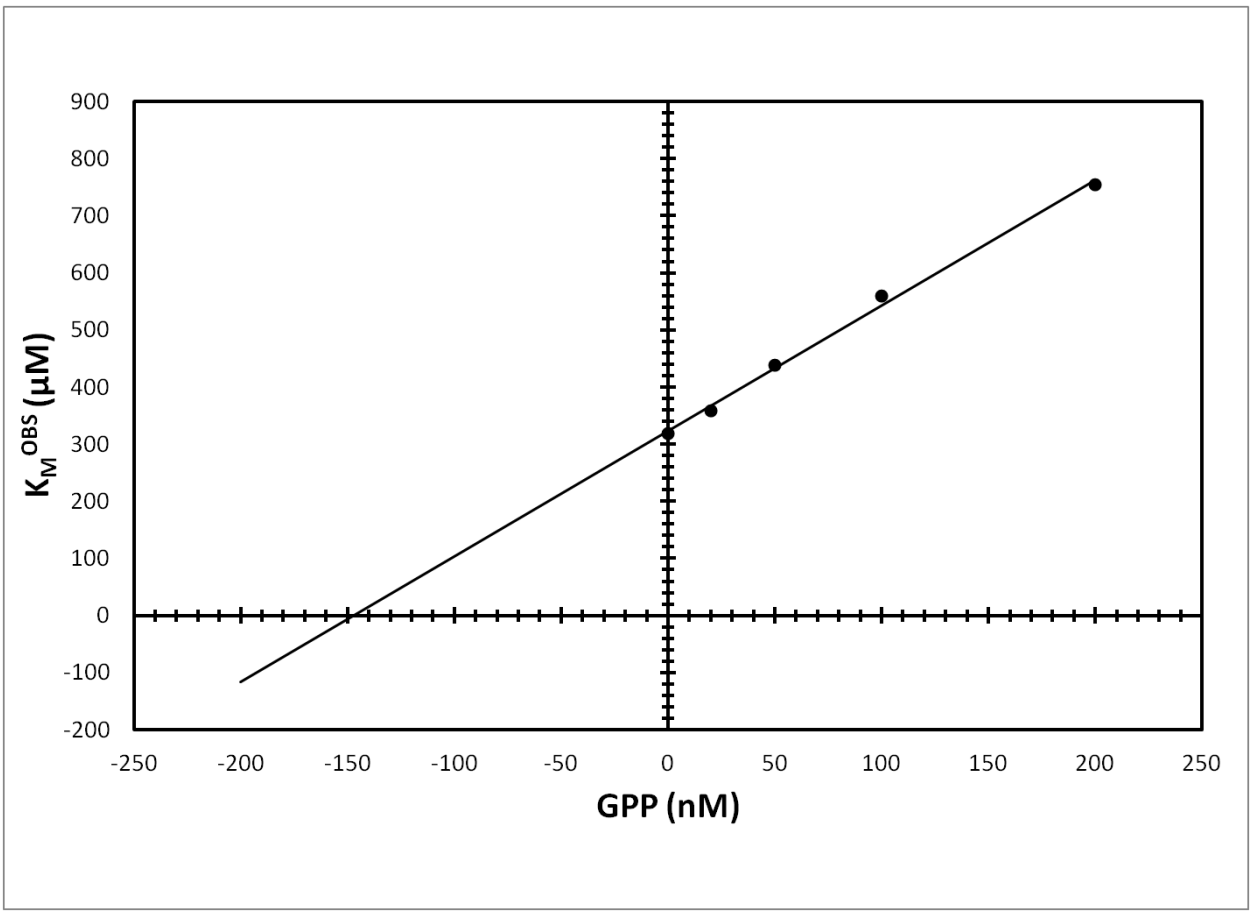

Figure 12. The K_i for geranyl pyrophosphate on mevalonate kinase is 147 ± 6 nM.

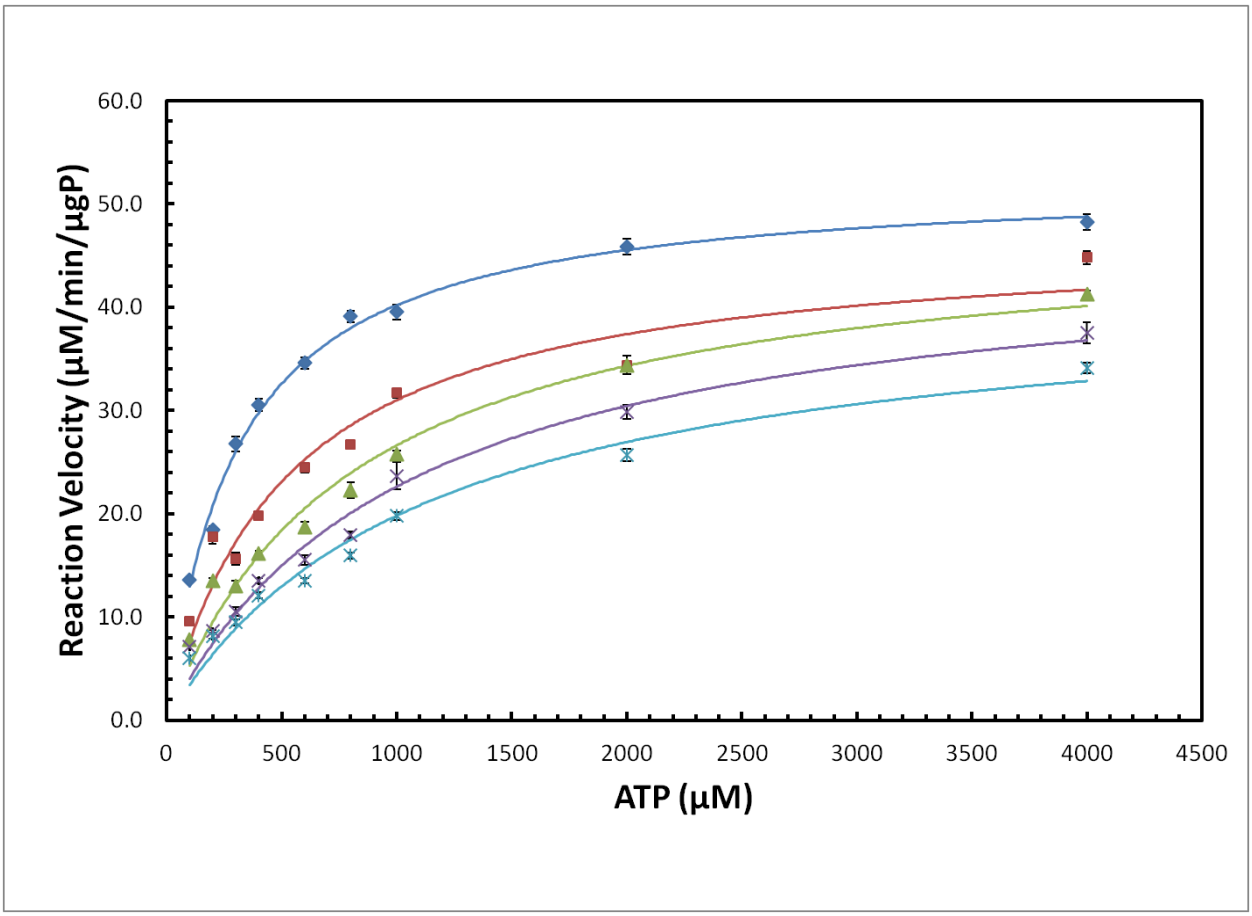

Figure 13. Competitive inhibition of mevalonate kinase by geranylgeranyl pyrophosphate at 0 nM (dark blue), 200 nM (red), 400 nM (green), 600 nM (purple), and 800 nM (light blue).

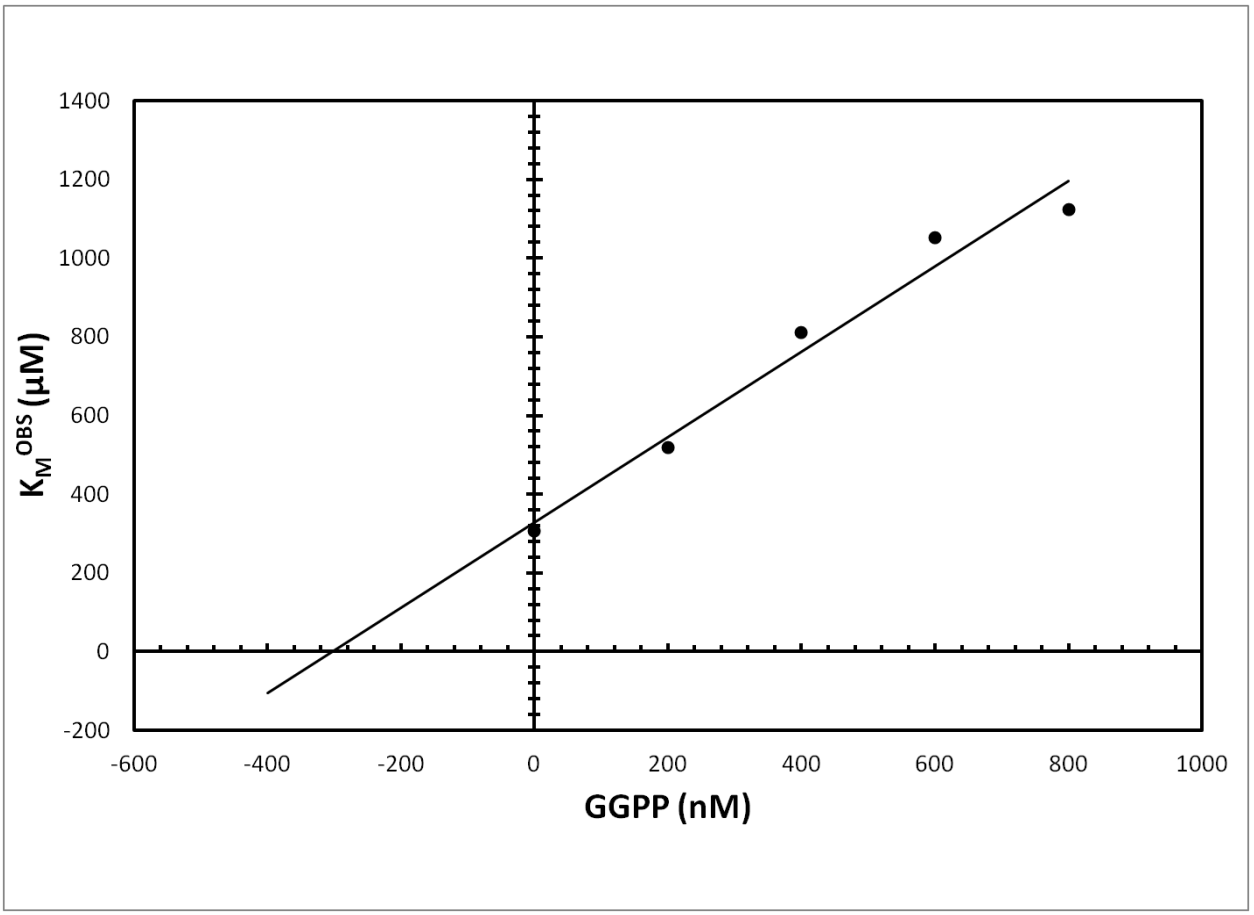

Figure 14. The K_i for geranylgeranyl pyrophosphate on mevalonate kinase is 303 ± 64 nM.

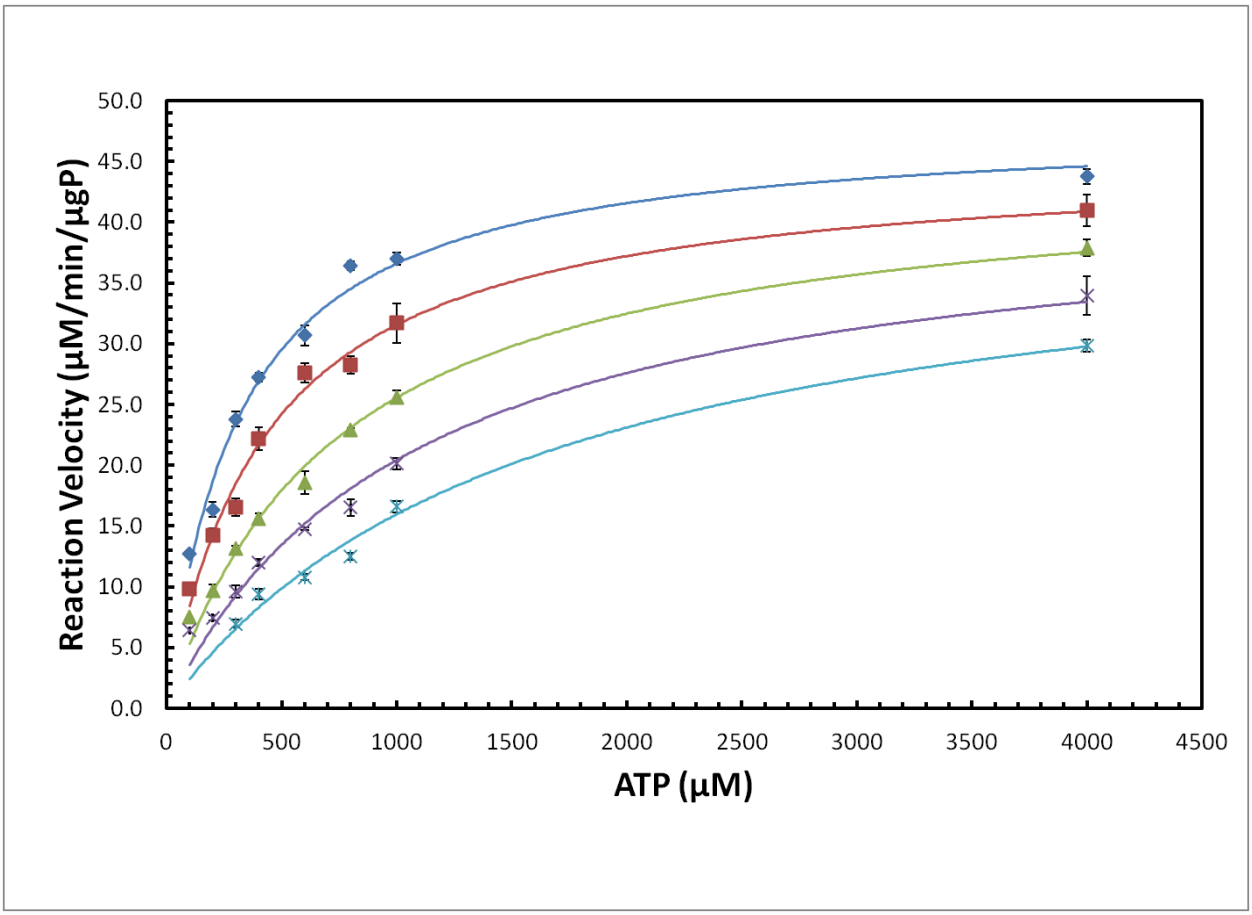

Figure 15. Competitive inhibition of mevalonate kinase by dimethylallyl pyrophosphate at 0 µM (dark blue), 5 µM (red), 25 µM (green), 50 µM (purple), and 100 µM (light blue).

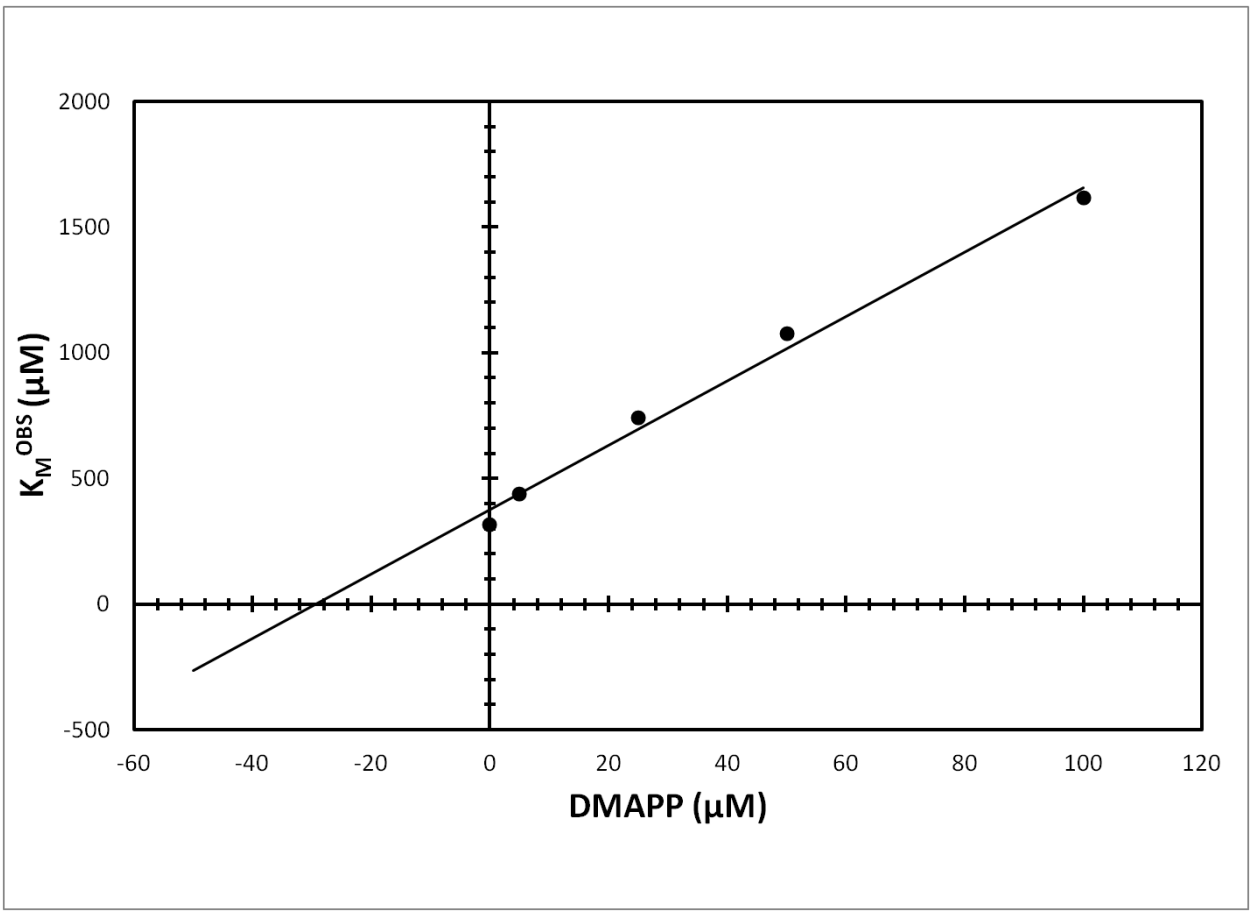

Figure 16. The K_i for dimethylallyl pyrophosphate on mevalonate kinase is 29 ± 5 µM.

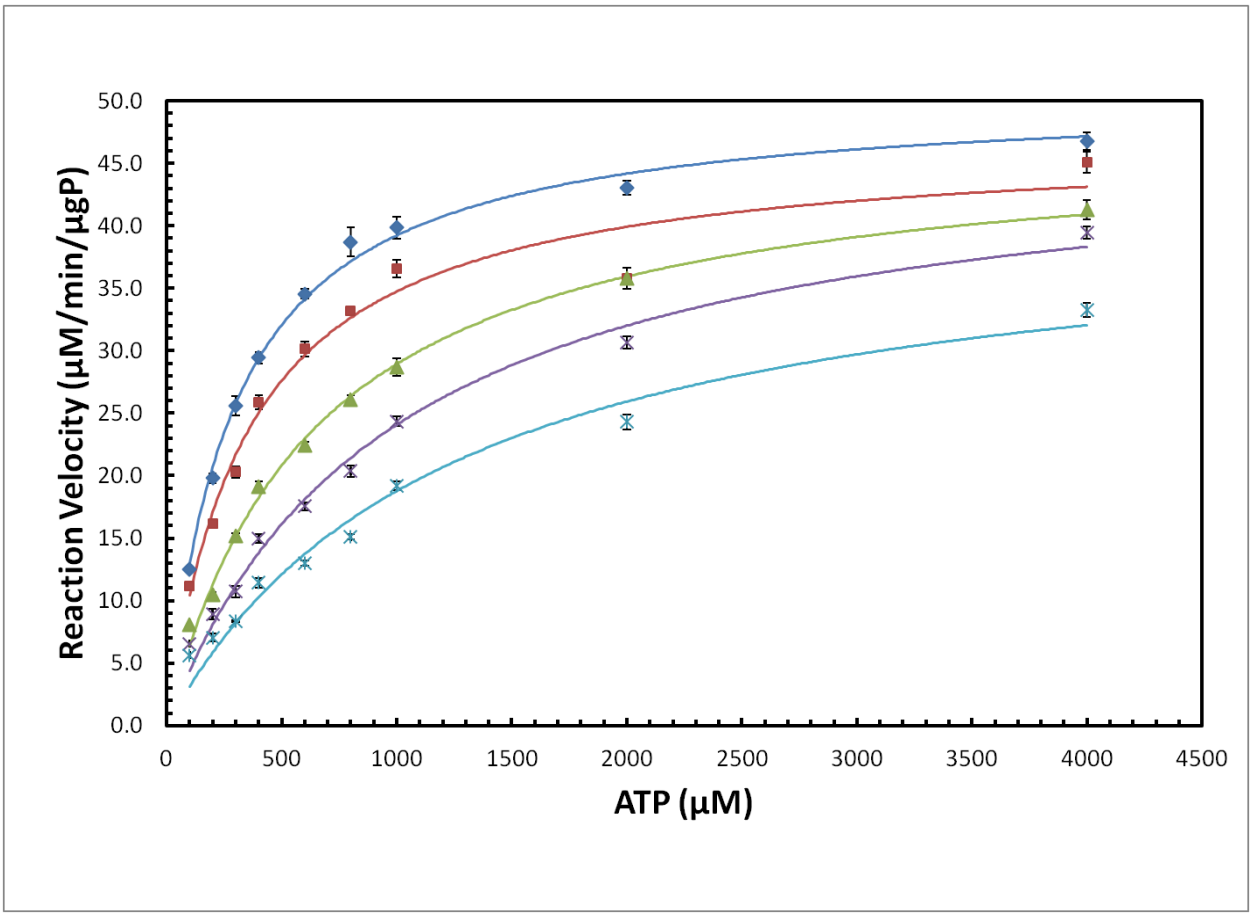

Figure 17. Competitive inhibition of mevalonate kinase by isopentenyl pyrophosphate at 0 µM (dark blue), 5 µM (red), 25 µM (green), 50 µM (purple), and 100 µM (light blue).

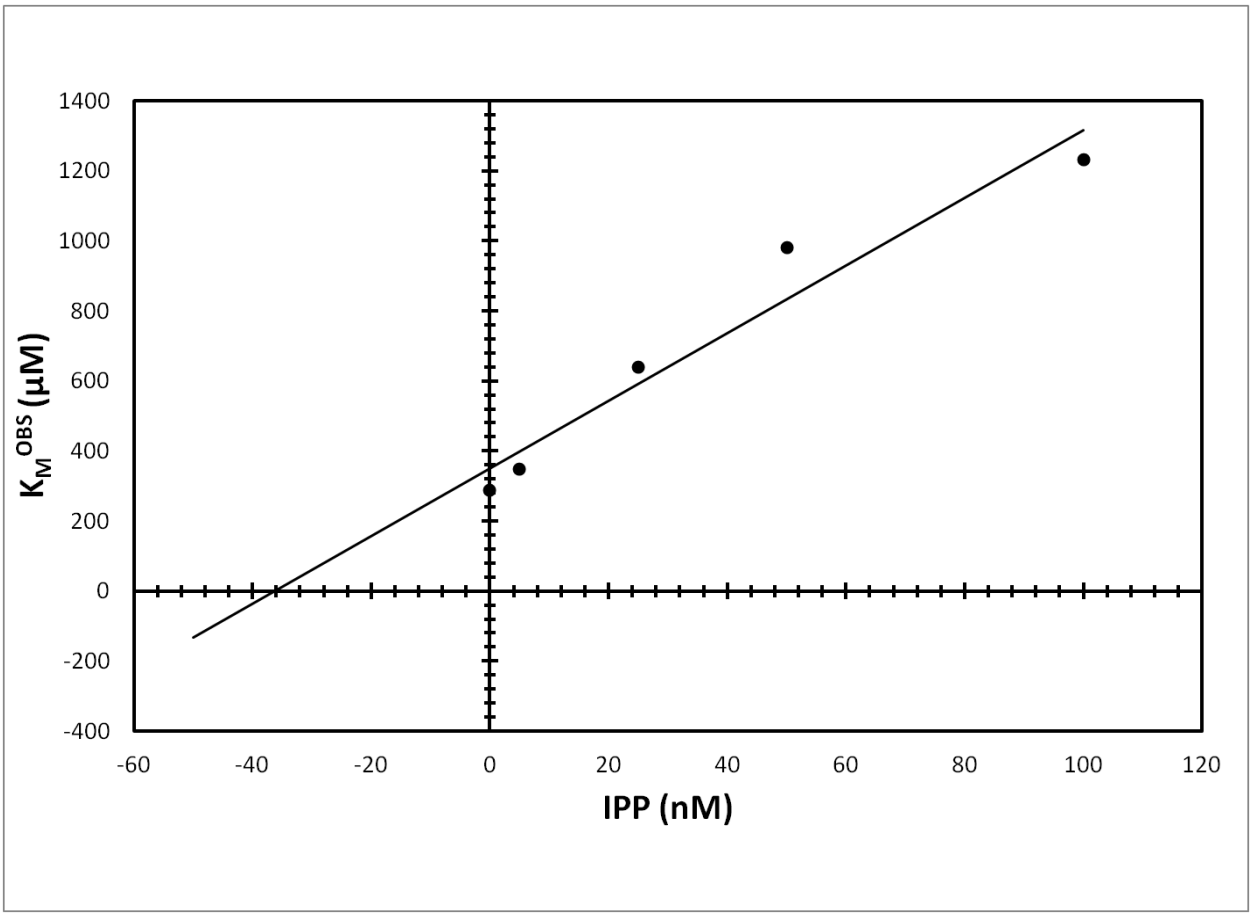

Figure 18. The K_i for isopentenyl pyrophosphate on mevalonate kinase is 36 ± 12 µM.

We also tested MK derived from *M. mazei*¸ which also had not been characterized at the onset of this work, but whose characterization was published simultaneously with *S. cerevisiae* derived MK (Primak*, et al.*, 2011). We determined the K_M^{ATP} to be 2.0 ± 0.5 mM and the v_{max} of the enzyme to be 69 ± 4 µM/min/µgE (or k_{cat} = 56 ± 4 s^{-1}) (Figure 19). Although the statistical analysis of the data showed that FPP was not an inhibitor of *M. mazei* MK up to 50 µM, based on a cursory view of the nonlinear regression analysis plot it is tempting to think otherwise. If one analyzes the data via the Lineweaver-Burk method, the lack of inhibition becomes clear (Figure 20). We also tested IPP for inhibitory affects on *M. mazei* MK and found that it had none up to 50 µM (Figure 21).

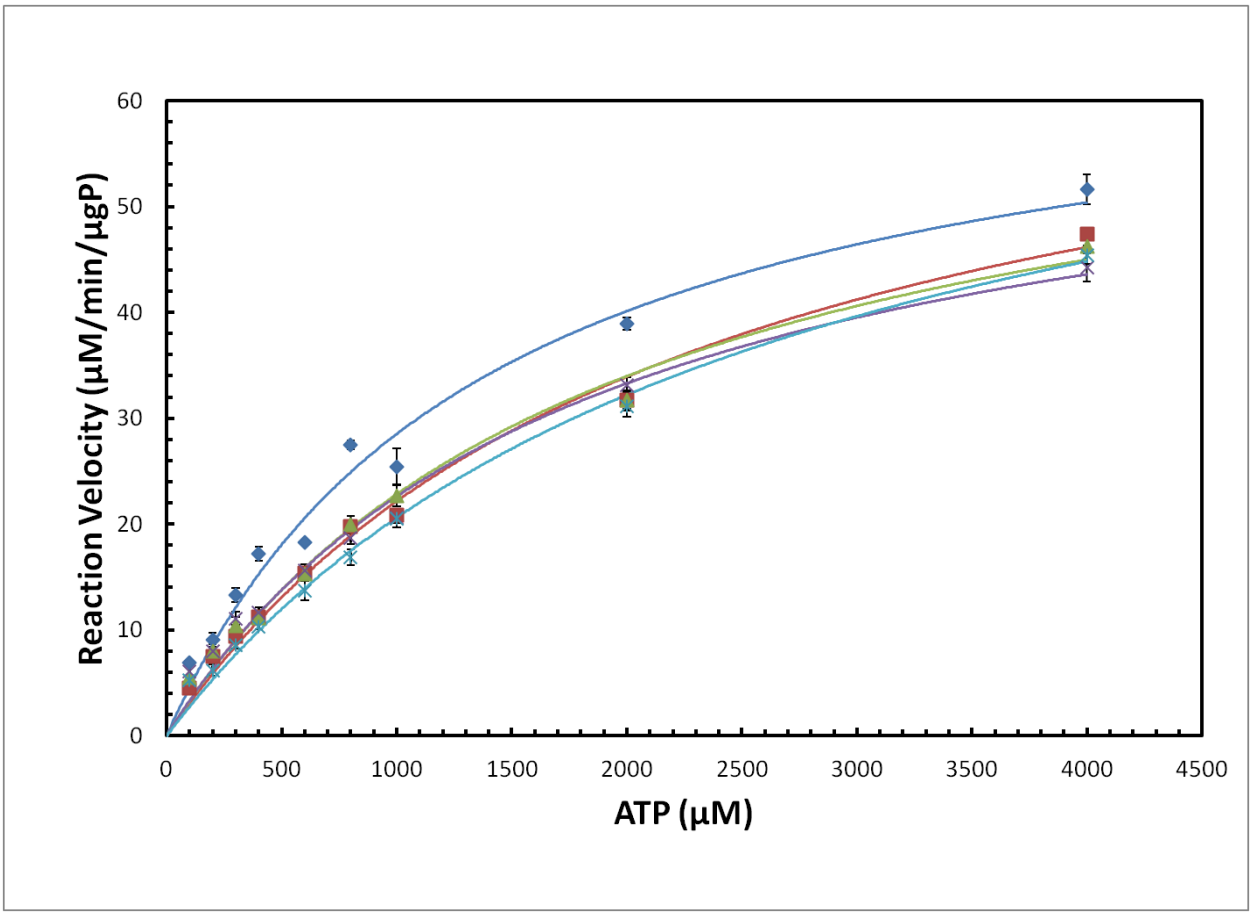

Figure 19. For *M. mazei* derived MK, K_M^{ATP} = 2.0 ± 0.5 mM, v_{max} = 69 ± 4 µM/min/µgE (or k_{cat} = 56 ± 4 s^{-1}), and the enzyme is not inhibited FPP.

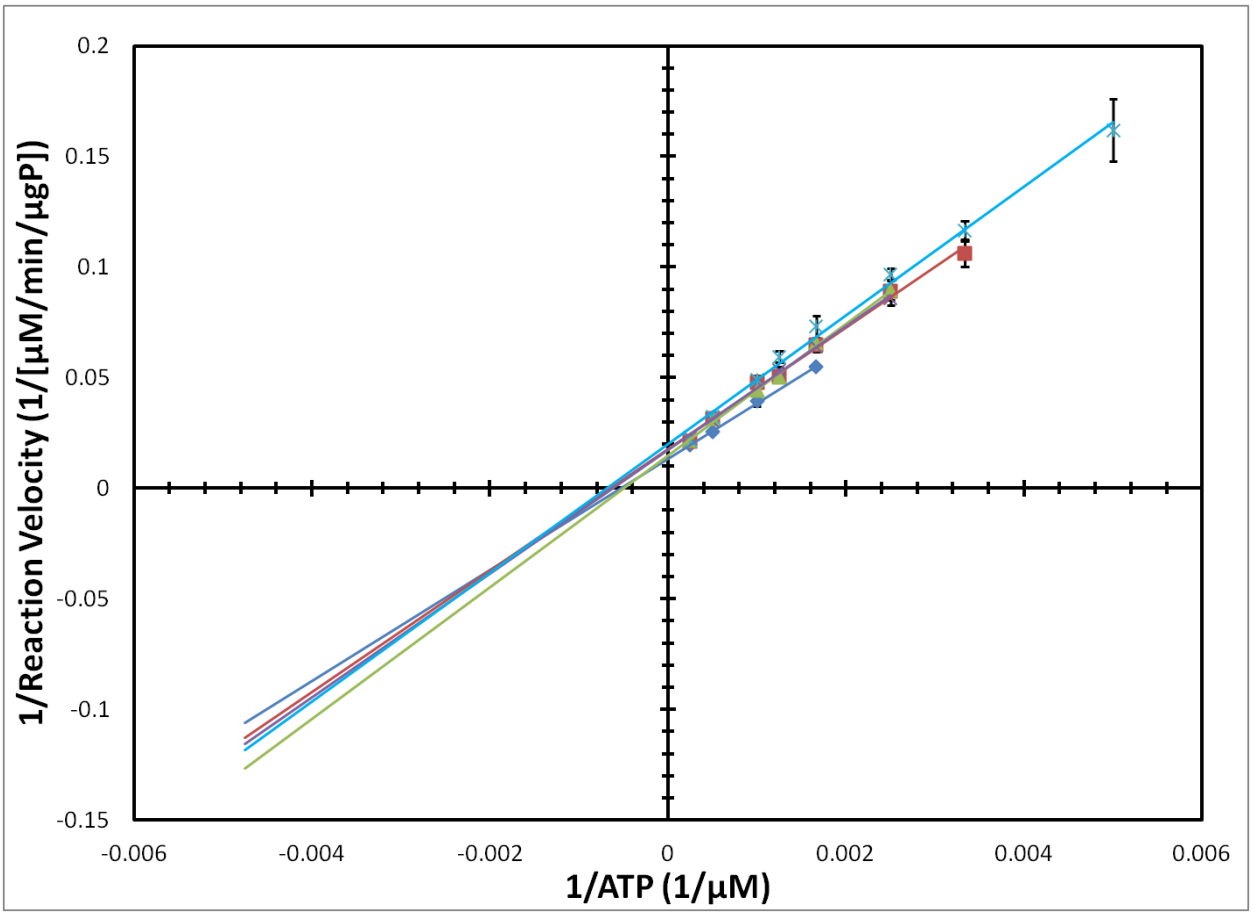

Figure 20. A Lineweaver-Burk analysis showing that FPP does not inhibit *M. mazei* MK at concentrations up to 50 µM. FPP concentrations: 0 µM (dark blue), 10 µM (red), 25 µM (green), 35 µM (purple), and 50 µM (light blue).

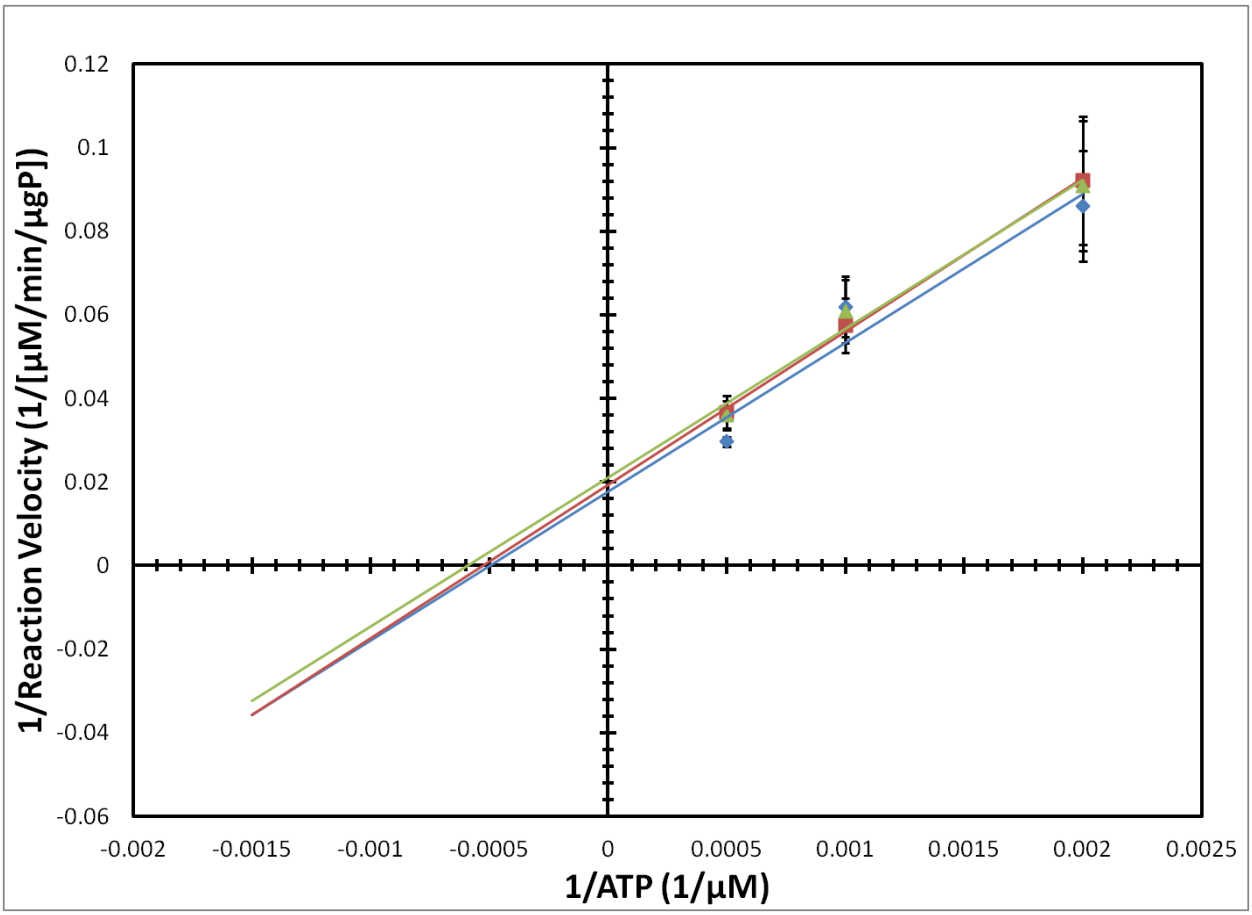

Figure 21. A Lineweaver-Burk analysis showing that IPP does not inhibit *M. mazei* MK at concentrations up to 50 µM. IPP concentrations: 0 µM (dark blue), 10 µM (red), 50 µM (green).

Given that *M. mazei* MK is not inhibited by the two isoprenoids we tested, nor any others (Primak*, et al.*, 2011), substituting it for *S. cerevisiae* MK in the heterologous mevalonate pathway being used to produce advanced biofuels might be advantageous. However, it is important to keep in mind that ${}^{ATP}K_M$ for *M. mazei* MK is very high given that it is in the millimolar range. It may be the case that different organisms have had to evolve different mechanisms for tightly regulating MK. Whether it is by both substrate and feedback inhibition in *S. cerevisiae* or poor binding in *M. mazei*, MK might be a bottleneck in the production on biofuels that cannot itself be engineered, but instead must be engineered around.

3.3 Materials and Methods

Codon Optimization of MK

The original *S. cerevisiae* MK sequence, which was downloaded from the BioCyc.org database, was codon optimized by DNA2.0 (Menlo Park, CA) for expression in *E. coli* (Appendix, Table 2).

M. mazei MK Expression Plasmid Construction

The plasmid pPro296_MK contained *M. mazei* derived MK codon-optimized for expression in *E. coli* and was a gift from Kevin George (Joint BioEnergy Institute).

S. cerevisiae MK Expression Plasmid Construction

A chemically-competent strain of *E. coli* DH10B was transformed with pET-30a+ (Novagen, Germany) and then used to prepare the plasmid according to the instructions and materials in a Qiagen (Valencia, California) Spin Miniprep Kit. The codon-optimized MK sequence was PCR amplified with primers that added an NdeI restriction site and a 6H-tag on the 5' end of the sequence and an XhoI restriction site on the 3' end of the sequence, then digested with the appropriate restriction enzymes (all enzymes from New England BioLabs, Ipswich, Massachusetts), and cloned into pET-30a+ to make expression plasmid pET-30a+_co2MK-NH. Confirmation of expression plasmid construction was accomplished by sequencing the cloning region using T7 primers (sequencing and primers from Quintara Biosciences, Albany, California).

M. mazei MK-His Expression and Purification

Conditions for ideal MK expression were screened on NuPAGE 10% Bis-Tris SDS-PAGE gels and the supplies indicated in the accompanying protocol (Invitrogen, Grand Island, New York) from 5-mL cultures that spanned a range of media types, growth temperatures, inducer concentrations, and growth times. Protein expression was ultimately accomplished by growing a 100-mL culture in Luria Broth (Invitrogen) to OD_{600} = 0.6 at 30 °C, inducing with 20 mM sodium propionate (Sigma Aldrich, St. Louis, Missouri), then growing overnight (until stationary phase was reached). The cells were pelleted and re-suspended in 25 mL of a lysis buffer (10 mM Imidazole, 300 mM NaCl, 50 mM NaH_2PO_4, pH = 8.0; Sigma Aldrich), sonicated for 10 minutes in a water bath to break up residual clumps, then homogenized with two passes through an EmulsiFlex®-C3 (Avestin, Canada). Cell debris was removed by centrifugation at 12,000 X g for 30 minutes. Cleared lysate was bound to 2-mL of Ni-NTA resin (Qiagen) at 4 °C by rocking gently for 30 minutes. The resin was then bedded in a column, washed with 20 column volumes (CV) of buffer containing 20 mM imidazole, then the protein was eluted with 10 CV of buffer containing 500 mM imidazole. Buffer exchange into 20 mM Tris, 50 mM NaCl, pH = 7.0 was accomplished on an AKTA (GE Healthcare Life Sciences, Pittsburgh, Pennsylvania) using a GE Healthcare HiPrep 26/10 Desalting Column (17-5087-01). Protein was then concentrated using VivaSpin 20 3,000-MWCO filters (Sartorius, Bohemia, New York). Protein

concentration was determined using a Nanodrop (Thermo Scientific, West Palm Beach, Florida). The protein was then diluted so that glycerol (Sigma) was 50% v/v and stored at -20 °C.

S. cerevisiae MK-His Expression and Purification

Conditions for ideal MK expression were screened on NuPAGE 10% Bis-Tris SDS-PAGE gels and the supplies indicated in the accompanying protocol (Invitrogen, Grand Island, New York) from 5-mL cultures that spanned a range of media types, growth temperatures, inducer concentrations, and growth times. Protein expression was ultimately accomplished by growing a 1-L culture in Terrific Broth (Invitrogen) to OD_{600} = 0.6 at 37 °C, inducing with 100 µM IPTG (Sigma Aldrich, St. Louis, Missouri), then growing at 25 °C for overnight (until stationary phase was reached). Cells were pelleted in 250-mL portions, flash frozen in liquid nitrogen after medium removal, and then stored at -80 °C prior to further processing. On ice, cells from one 250-mL portion were suspended in 25 mL of a lysis buffer (10 mM Imidazole, 300 mM NaCl, 50 mM NaH_2PO_4, pH = 8.0; Sigma Aldrich), sonicated for 10 minutes in a water bath to break up residual clumps, then homogenized with two passes through an EmulsiFlex®-C3 (Avestin, Canada). Cell debris was removed by centrifugation at 12,000 X g for 30 minutes. Cleared lysate was bound to 2-mL of Ni-NTA resin (Qiagen) at 4 °C by rocking gently for 30 minutes. The resin was then bedded in a column, washed with 20 column volumes (CV) of buffer containing 20 mM imidazole, then the protein was eluted with 10 CV of buffer containing 500 mM imidazole. Buffer exchange into 20 mM Tris, 50 mM NaCl, pH = 7.0 was accomplished on an AKTA (GE Healthcare Life Sciences, Pittsburgh, Pennsylvania) using a GE Healthcare HiPrep 26/10 Desalting Column (17-5087-01). Protein was then concentrated using VivaSpin 20 3,000-MWCO filters (Sartorius, Bohemia, New York). Protein concentration was determined using a Nanodrop (Thermo Scientific, West Palm Beach, Florida). The protein was then diluted so that glycerol (Sigma) was 50% v/v and stored at -20 °C.

Activity Assay

All chemicals and supporting enzymes were purchased from Sigma-Aldrich. Reaction progress was monitored spectrophotometrically at 339 nm for NADH consumption on a 96-well plate in a Spectramax M2 (Molecular Devices, Sunnyvale, California). Mevalonate was made by the saponification of mevalonolactone with KOH at 3:1 (mol:mol) KOH:mevalonolactone for 2 hours at 37 °C, 200 rpm. Conversion was verified via normal phase TLC developed in isopropanol and stained with basic permanganate, and titrated to pH = 7.0. 100-µL enzymatic assay mixtures contained 200 mM Tris (pH = 7.2), 100 mM KCl, 10 mM MgCl2, 0.81 mM NADH, 1.5 mM phosphoenolpyruvate, 2.8 mM mevalonate, 0.682U pyruvate kinase, 0.990 U lactate dehydrogenase, and 0.1 µg MK, 0.1-4.0 mM ATP, and were maintained at 30 °C. When examining feedback inhibition, the same reaction conditions were used from before with the addition of one of the following: 0-100 nM FPP, 0-200 nM GPP, 0-800 nM GGPP, 0-100 µM IPP,

or 0-100 µM DMAPP. Stock concentrations of NADH and pH-neutralized ATP were confirmed through their extinction coefficients ($^{ATP}\varepsilon_{259nm}$ = 15.4 $mM^{-1}cm^{-1}$, $^{NADH}\varepsilon_{339nm}$ = 6.22 $mM^{-1}cm^{-1}$). All conditions were repeated six times for statistical analysis, from which K_M (µM) and reaction velocities (µM mev-p formed*$minute^{-1}$ * µg MK^{-1}) were calculated using nonlinear regression analysis via the solver function in Excel (Microsoft). To ensure MK was the rate-limiting enzyme, when necessary the following standard controls and results were verified: doubling the MK added doubled the observed rate, doubling the supporting enzymes added did not affect the observed rate, and doubling the phosphoenolpyruvate concentration did not affect the observed rate.

Chapter 4. The expression, purification, and kinetic characterization of phosphomevalonate kinase from *Saccharomyces cerevisiae*[2]

4.1 Introduction

The mevalonate pathway is an important conduit for the production of crucial metabolites with a wide array of functions, including terpenoids (Wilding*, et al.*, 2000, Kuzuyama, 2002), hormones and steroids (Kuzuyama & Seto, 2012). The heterologous expression of this pathway in *Escherichia coli* has enabled high-level production of the antimalarial drug artemisinin (Martin*, et al.*, 2003, Ro*, et al.*, 2006, Chang*, et al.*, 2007), but the chemical structures of these metabolites also make them interesting targets for solving some of the most crucial problems in the energy market (Bokinsky*, et al.*, 2011, Peralta-Yahya*, et al.*, 2011). With only slight modifications to mevalonate pathway intermediates and products, either *in vivo* or through traditional chemical engineering processes post cell culture extraction, these molecules can be transformed into biofuels that, depending on our ability to scale-up, could offset or replace traditional liquid fuels (Zhang*, et al.*, 2011). This would allow us to replace petroleum-based, CO_2 producing fuels with fuels that are carbon neutral. Although industrial-scale corn-based ethanol production is already a reality in the energy market, ethanol is a less than desirable biofuel because not only does it divert crops from the food supply, it is not compatible with our current distribution infrastructure or vehicle fleet (Lee*, et al.*, 2008).

Whether these fuel alternatives are five-carbon alcohols derived from the mevalonate pathway intermediates isopentenyl pyrophosphate and dimethylallyl pyrophosphate (Chou & Keasling, 2011), or downstream, terpene-based molecules like bisabolene (Peralta-Yahya*, et al.*, 2011), further improvement of titers may be realized through a more robust understanding of the enzymes in the mevalonate pathway and the ways in which those enzymes are regulated by metabolic intermediates. In particular, proteomics data has previously shown that the fourth and fifth enzymes in the pathway—mevalonate kinase (MK) and phosphomevalonate kinase (PMK), respectively—are expressed at relatively low levels and may be targets for increasing overall fuel production (Redding-Johanson*, et al.*, 2011, Singh*, et al.*, 2012). Previous work has also shown that substrate inhibition and feedback inhibition of MK may be responsible for limiting flux through the pathway (Ma*, et al.*, 2011). Because MK—a phosphotransferase that acts on mevalonate and ATP to yield mevalonate-5-phosphate—and PMK—a phosphotransferase that acts on mevalonate-5-phosphate and ATP to yield mevalonate-5-diphosphate—both require ATP to function and downstream prenyl phosphates might act as

[2] The contents of this chapter have been submitted for publication, but have been neither accepted nor rejected at the time of filing.

general ATP binding site inhibitors, PMK was identified as another potential source of pathway regulation.

PMKs from other sources have been studied revealing implications for pathway engineering. For example, PMK from *E. faecalis* is Mn^{2+} dependent rather than Mg^{2+} dependent (Doun*, et al.*, 2005). Pig-derived PMK is substrate inhibited by ATP under high ATP, low mevalonate phosphate concentrations (Eyzaguirre*, et al.*, 2006). If *S. cerevisiae* PMK is similarly dependent or inhibited it would make an ideal target for protein engineering. Furthermore, *S. cerevisiae* prefers to grow at 30 °C, but much of our production takes place in *E. coli*, which necessitates understanding how PMK activity is affected by a change in growth temperature from 30 °C to 37 °C. Herein we report cloning a codon-optimized sequence of *S. cerevisiae* PMK into an expression vector, the expression and purification of PMK in *E. coli*, and the kinetic characterization of the purified enzyme.

4.2 Results and Discussion

Although PMK from *S. cerevisiae* has previously been studied in partially purified lysates (Bloch*, et al.*, 1959), and even utilized to study the kinetics of another enzyme (Primak*, et al.*, 2011), this is the first time PMK from *S. cerevisiae* has been kinetically characterized in isolation. In a study of the partially purified enzyme it was reported that pH did not affect PMK activity, but we have found that PMK does have an optimal activity at pH = 7.2, and activity drops off below pH = 6.5 and above pH = 8.0 (Figure 22). Although at first glance there is an apparent "shoulder" in the pH profile, careful consideration of the profile graph shows that the shoulder is within error and therefore cannot be considered to conclusively exist. Although we did not test a wide array of storage conditions, solutions with high PMK concentrations were found to be stable long term only at pH = 8.0 with 800 mM NaCl. As found previously *S. cerevisiae* PMK shows a cation dependence on Mg^{2+}, with 10 mM corresponding to maximal activity (Figure 23).

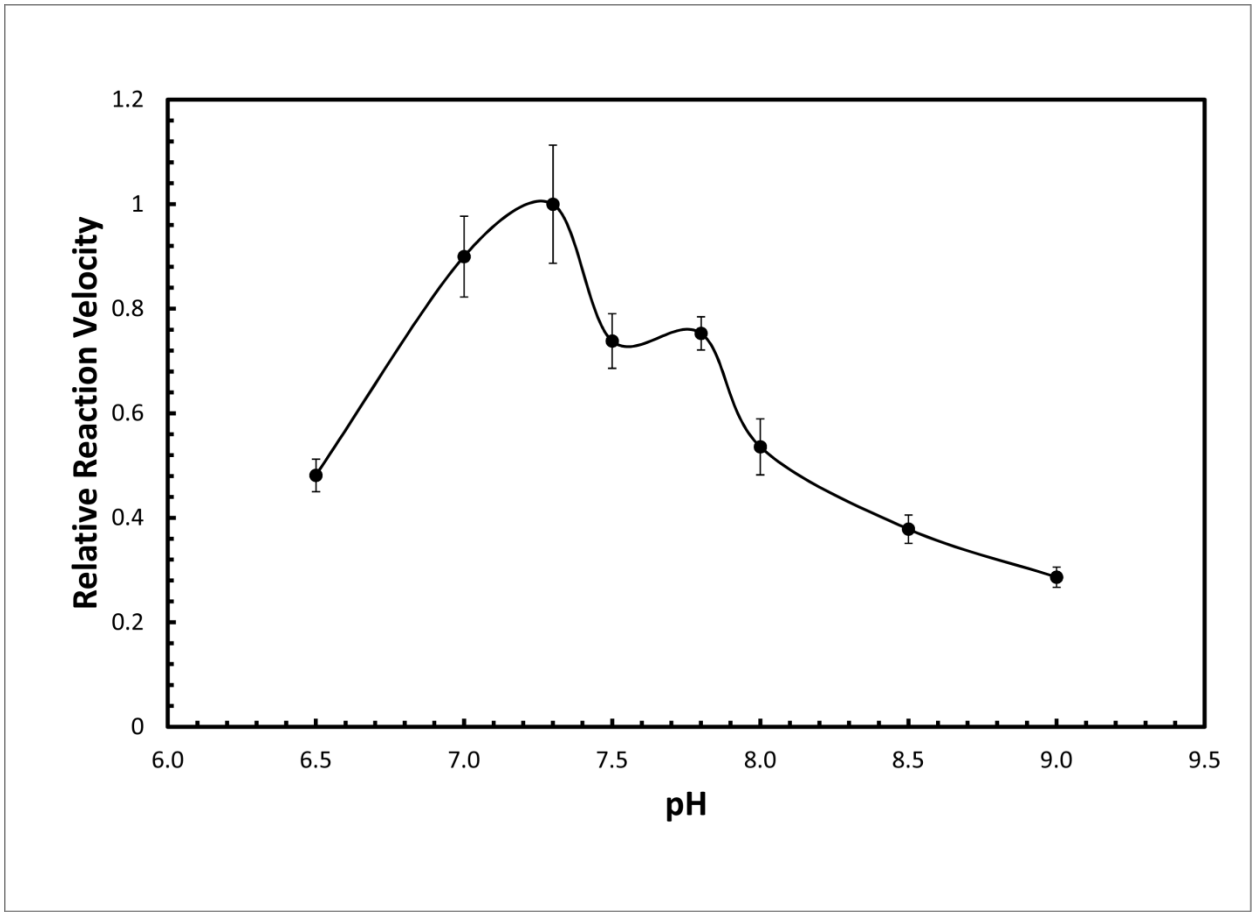

Figure 22. pH dependence of *S. cerevisiae* phosphomevalonate kinase.

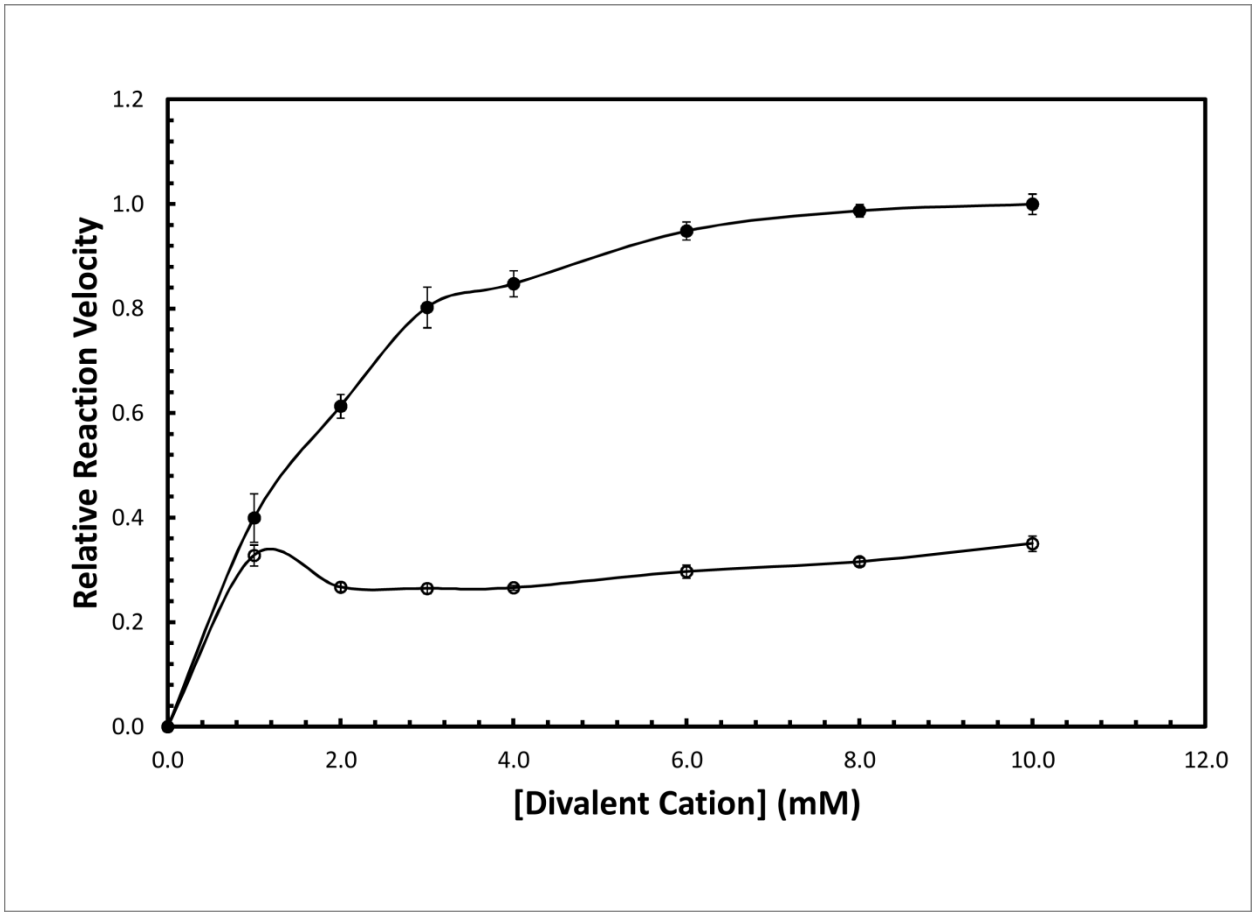

Figure 23. Divalent cation dependence. Closed circles are data for Mg^{2+} and open circles are data for Mn^{2+}.

Kinetic constants were determined by nonlinear regression analysis using the solver function in MS Excel. K_M^{ATP} was determined to be 98.3 µM and 74.3 µM at 30 °C and 37 °C, respectively. $K_M^{mev\text{-}p}$ was determined to be 885 µM and 880 µM at 30 °C and 37 °C, respectively (Figure 24). v_{max} was determined to be 45.1 µmol/min/µgE and 53.3 µmol/min/µgE at 30 °C and 37 °C, respectively (Figure 25). Because this enzyme has been used heterologously in *E. coli* for production of isoprenoids (Martin*, et al.*, 2003, Ro*, et al.*, 2006, Chang*, et al.*, 2007, Bokinsky*, et al.*, 2011, Chou & Keasling, 2011, Peralta-Yahya*, et al.*, 2011), the temperature effect on PMK activity is important, particularly at *E. coli*'s optimal growth temperature of 37 °C. Despite expectations that PMK activity might diminish with increasing the temperature from the preferred 30 °C growth temperature of *S. cerevisiae* to the 37 °C preferred by *E. coli*, PMK activity was shown to slightly increase with the increase in temperature. This increased activity bodes well for the production of isoprenoid products, including advanced biofuels, via the mevalonate pathway if the low protein expression levels currently observed can be increased (Redding-Johanson*, et al.*, 2011, Singh*, et al.*, 2012). It should be noted that although we were able to achieve very high yields of PMK using pET-52b+ for the purpose of isolating and

purifying the enzyme, increasing PMK expression in production strains by using high copy plasmids would be counterproductive to increasing overall biofuels production as doing so would divert an unnecessary amount of resources into the production of protein to the detriment of fuel titers.

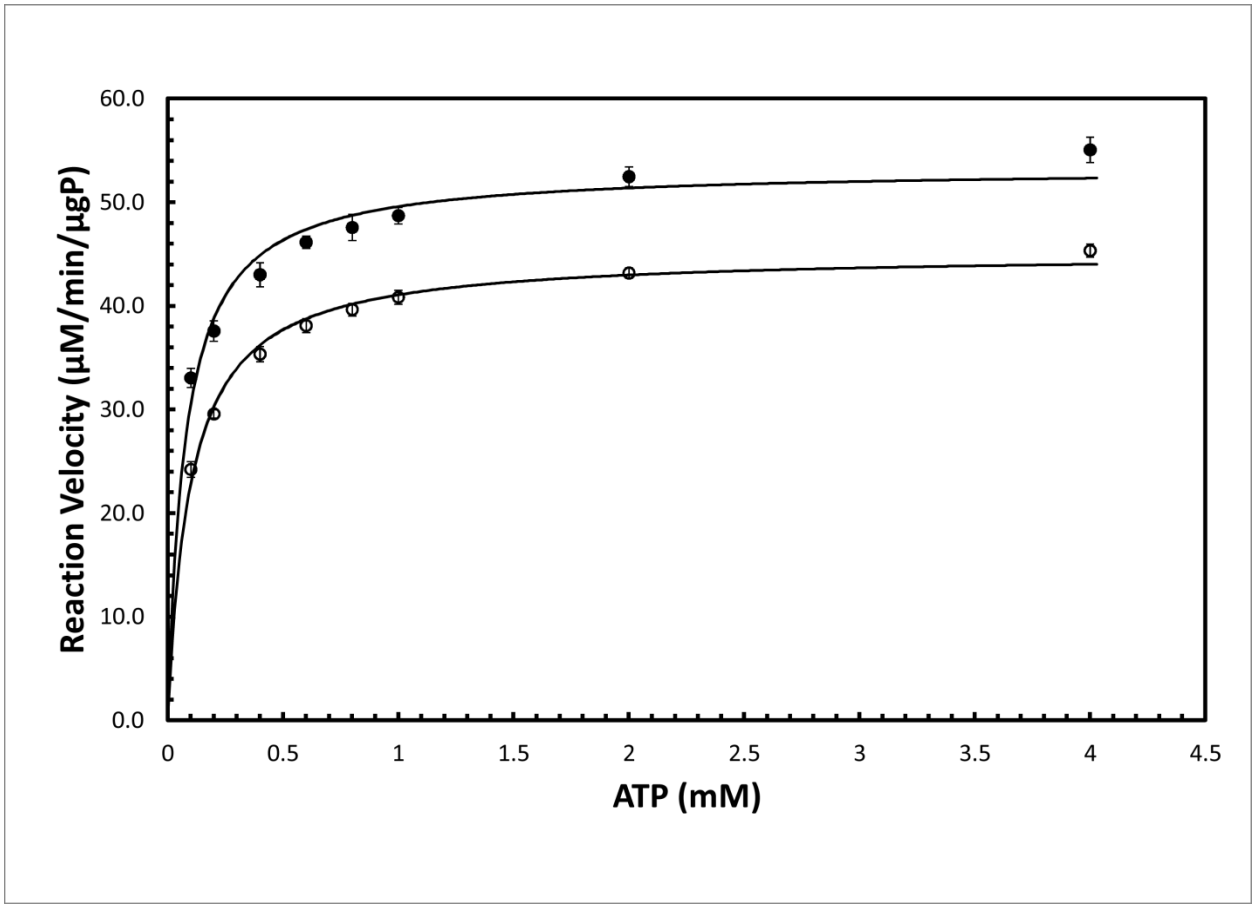

Figure 24. Initial reaction velocity as a function of ATP concentration. Closed circles are data for incubation at 37 °C and open circles are data for incubation at 30 °C.

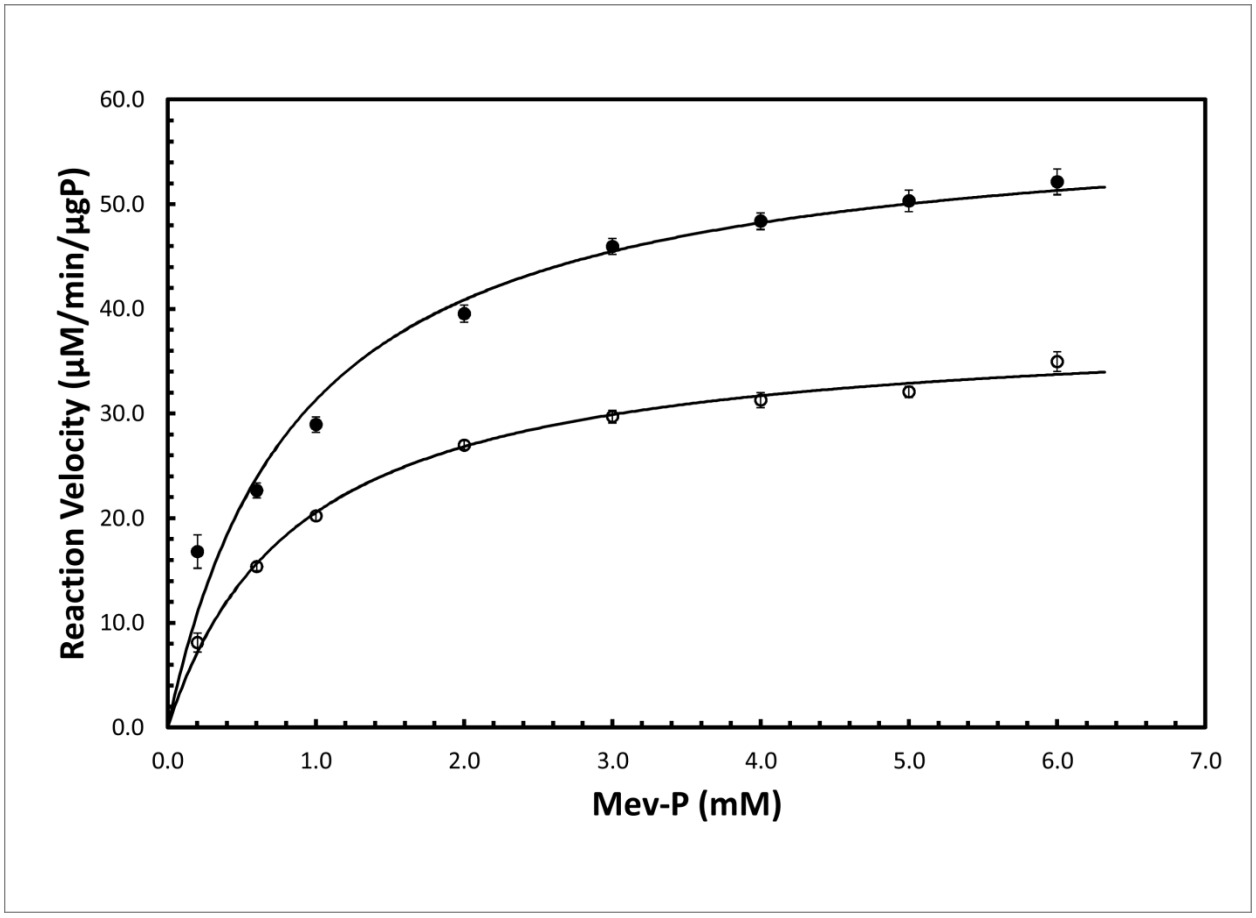

Figure 25. Initial reaction velocity as a function of mevalonate-5-phosphate concentration. Closed circles are data for incubation at 37 °C and open circles are data for incubation at 30 °C.

The K_M for the ATP binding site is 74.3 µM at 37 °C, a full order of magnitude lower than the K_M (880 µM at 37 °C) for the mevalonate-5-phosphate (mev-p) binding site. Despite the fact that the maximum reaction velocity of the enzyme is fast, PMK has a low catalytic activity (being much less sensitive to the presence of mev-p), which might be one important way that PMK and the mevalonate pathway are regulated. One regulatory mechanism for controlling PMK activity we can rule out is feedback inhibition, as the presence of farnesyl pyrophosphate (FPP)—a known inhibitor of MK (Primak*, et al.*, 2011)—did not affect PMK activity at concentrations up to 10 µM FPP (data not shown). Unlike *S. cerevisiae* mevalonate kinase (Primak*, et al.*, 2011), PMK did not demonstrate substrate inhibition. Although the lack of feedback and substrate inhibition is promising for using *S. cerevisiae* PMK to increase biofuel titers, the use of *S. cerevisiae* derived PMK should probably be abandoned for more active PMKs from other sources, such as *E. faecalis* (Doun*, et al.*, 2005), *pig liver* (Eyzaguirre*, et al.*, 2006), or *S. pneumonia* (Pilloff*, et al.*, 2003), because the $K_M^{mev\text{-}p}$ is quite high. It is likely that PMK is reversible, but given the poor characteristics of the forward PMK kinetics it is not worth

pursuing. Rather, *S. pneumonia* PMK is a much better enzyme and should be incorporated into future production strains.

With the addition of PMK from this study, the *S. cerevisiae*-derived mevalonate pathway enzymes that have been kinetically characterized include hydroxymethylglutaryl synthase (Middleton, 1972), hydroxymethylglutaryl reductase (Ma*, et al.*, 2011), mevalonate kinase (Primak*, et al.*, 2011), phosphomevalonate decarboxylase (Krepkiy & Miziorko, 2004), and farnesyl pyrophosphate synthase (Song, 1994), leaving acetyl-CoA C-acetyltransferase and isopentenyl diphosphate isomerase uncharacterized. Although isopentenyl diphosphate isomerase has been isolated and studied (Anderson*, et al.*, 1989), the difficulty associated with detecting the isomerization of a single bond is likely why the kinetic constants have yet to be determined. In combination with traditional genetic engineering techniques, such as varying promoter strength, and newly developed technologies for varying expression, such as RBS calculators (Salis, 2011), studying the kinetics of these remaining enzymes should allow the metabolic production from engineered microbes to be optimized more rationally.

4.3 Materials and Methods

Codon Optimization of PMK

The original *S. cerevisiae* PMK sequence, which was downloaded from the BioCyc.org database, was codon optimized by DNA2.0 (Menlo Park, CA) for expression in *E. coli* (Appendix, Table 3).

Expression Plasmid Construction

A chemically-competent strain of *E. coli* DH10B was transformed with pET-52b+ (Novagen, Germany) and then used to prepare the plasmid according to the instructions and materials in a Qiagen (Valencia, California) Spin Miniprep Kit. The codon-optimized PMK sequence was PCR amplified with primers that added a BsaI restriction site with an NcoI overhang on the 5' end of the sequence and a SacI restriction site on the 3' end of the sequence, then digested with the appropriate restriction enzymes (all enzymes from New England BioLabs, Ipswich, Massachusetts), and cloned into pET-52b+ to make expression plasmid pET-52b+_coPMK-His. Confirmation of expression plasmid construction was accomplished by sequencing the cloning region using T7 primers (sequencing and primers from Quintara Biosciences, Albany, California).

PMK-His Expression and Purification

Ideal conditions for PMK expression were screened on NuPAGE 10% Bis-Tris SDS-PAGE gels and the supplies indicated in the accompanying protocol (Invitrogen, Grand Island, New York) from 5-mL cultures that spanned a range of media types, growth temperatures, inducer concentrations, and growth times. Protein expression was ultimately accomplished by growing a 2-L culture in Terrific Broth (Invitrogen) to OD_{600} = 0.6 at 37 °C, inducing with 100 µM IPTG (Sigma Aldrich, St. Louis, Missouri), then growing at 18 °C for approximately two days (until stationary phase was reached). Cells were pelleted in 250-mL portions, flash frozen in liquid nitrogen after medium removal, and then stored at -80 °C prior to further processing. On ice, cells from one 250-mL portion were suspended in 25 mL of a lysis buffer (10 mM Imidazole, 300 mM NaCl, 50 mM NaH_2PO_4, pH = 8.0; Sigma Aldrich), sonicated for 10 minutes in a water bath to break up residual clumps, then homogenized with two passes through an EmulsiFlex®-C3 (Avestin, Canada). Cell debris was removed by centrifugation at 12,000 X g for 30 minutes. Cleared lysate was bound to 2-mL of Ni-NTA resin (Qiagen) at 4 °C by rocking gently for 30 minutes. The resin was then bedded in a column, washed with 20 column volumes (CV) of buffer containing 20 mM imidazole, then the protein was eluted with 10 CV of buffer containing 500 mM imidazole. Buffer exchange into 20 mM Tris, 50 mM NaCl, pH = 7.0 was accomplished on an AKTA (GE Healthcare Life Sciences, Pittsburgh, Pennsylvania) using a GE Healthcare HiPrep 26/10 Desalting Column (17-5087-01). Protein was then concentrated using VivaSpin 20 3,000-MWCO filters (Sartorius, Bohemia, New York). Protein concentration was determined using a Nanodrop (Thermo Scientific, West Palm Beach, Florida). The protein was then diluted so that glycerol (Sigma) was 50% v/v and stored at -20 °C.

Activity Assay

All chemicals and supporting enzymes were purchased from Sigma-Aldrich. Reaction progress was monitored spectrophotometrically at 339 nm for NADH consumption on a 96-well plate in a Spectramax M2 (Molecular Devices, Sunnyvale, California). 100-µL enzymatic assay mixtures contained 200 mM Tris (pH = 7.2), 100 mM KCl, 10 mM $MgCl_2$, 0.81 mM NADH, 1.5 mM phosphoenolpyruvate, 0.682U pyruvate kinase, 0.990 U lactate dehydrogenase, 0.1 µg PMK, 0.1-8.0 mM ATP, and 0.2-10.0 mM mevalonate-5-phosphate, and were maintained at either 30 °C or 37 °C. Stock concentrations of NADH and pH neutralized ATP were confirmed through their extinction coefficients ($^{ATP}\varepsilon_{259nm}$ = 15.4 $mM^{-1}cm^{-1}$, $^{NADH}\varepsilon_{339nm}$ = 6.22 $mM^{-1}cm^{-1}$). All conditions were repeated twelve times for statistical analysis, from which K_M (µM) and reaction velocities (µM mev-pp formed*$minute^{-1}$ * µg PMK^{-1}) were calculated using nonlinear regression analysis via the solver function in Excel (Microsoft). When studying pH effect and divalent cation dependence, ATP and mevalonate-5-phosphate were held constant and data were normalized to the maximum observed reaction velocities. To ensure PMK was the rate-limiting enzyme, when necessary the following standard controls and results were verified: doubling the PMK added doubled the observed rate, doubling the supporting enzymes added did not affect the observed rate, and doubling the phosphoenolpyruvate concentration did not affect the observed rate.

Chapter 5. Conclusion and future work

5.1 Conclusion

The goal of this study was to perform the kinetic characterization of two enzymes identified as potentially limiting our ability to increase biofuel production in *E. coli* via an engineered, heterologous metabolic pathway. This effort was successful in explaining why choosing a reversible HMGR, rather than an irreversible HMGR with a higher v_{max} or lower K_M, increased production titers. We also were able to confirm feedback inhibition of MK as a regulatory mechanism for controlling flux through the pathway. Inhibition of PMK was determined not exist, though the enzyme seems to have poor affinity for its substrate.

The big 'omics-focused research (i.e., genomics, proteomics, metabolomics, transcriptomics) that are now the cornerstone of synthetic biology provides a great deal of insight that was not available a decade ago and are in part responsible for the continued growth in understanding in the field. This study demonstrates, however, that it is still important to incorporate traditional biochemical studies into the complex endeavor of engineering metabolic pathways. While the research presented here has accomplished our intended goals, there is still more work that can be done to increase our understanding of our engineered pathway and the mechanisms by which we may be able to further push the limits of using microbes as living chemical factories.

5.2 Future Work

Mevalonate Kinase

The expression and purification of *S. cerevisiae* MK provided some insight into its structure making the crystallization of the protein an interesting future direction. In the first attempt to purify MK the six-histidine tag was added to the C-terminal end of the protein; although the protein expressed quite well as visualized via Coomassie stained SDS-PAGE (data not shown), under native conditions the enzyme could not be purified on Ni-NTA resin, indicating the C-terminus of MK has little or no solvent exposure. This trait, if confirmed, would make it different from other known eukaryotic MKs like human MK and rat MK. The structures of all known MKs closely align based on their phylogenetic origins—eukaryotic, bacterial, and archaeal—and these structures impart different regulatory mechanisms for enzyme activity. For example, it is generally the case that the binding sites in bacterial MKs have more solvent exposure and, thus, have less affinity toward those inhibitors at the binding site. Instead it appears that the activities of these enzymes are regulated by other means (e.g., transcriptional, substrate binding affinity, etc.). Given that eukaryotic MKs seem to be more inhibited by downstream metabolites because they have less solvent exposure at the active site, by crystallizing the protein it might be possible to determine which residues can be changed to shrink the size of the binding pocket, eliminating the ability of larger inhibitors from fitting into the binding site. Another possibility is to truncate the protein to increase solvent exposure of the binding site, which in turn might decrease the K_i values for the inhibitors. Having the structure of the protein potentially gives us the opportunity to alter residues to lower K_M values, which favors more turnover of substrate.

Another important aspect of determining the structure of MK is the substrate inhibition by mevalonate. As was previously discussed, there are a number of possible mechanisms for substrate inhibition (e.g., an allosteric binding site, a problematic residue in the binding pocket). Having the structure of the enzyme would help elucidate the mechanism of substrate inhibition and would inform efforts to mutate the protein to eliminate substrate inhibition.

Phosphomevalonate Kinase

Given that phosphomevalonate kinase (PMK) was not found to be feedback inhibited by any of the prenyl phosphates we tested, any future work on PMK it should be focused on engineering it to have a lower K_M for mev-p. The K_M we measured was quite high (885 µM and 880 µM at 30 °C and 37 °C, respectively) and calls into question whether it would function normally at typical cellular concentrations of mevalonate-5-phosphate (mev-p). In this case a structure would be helpful in determining which residues are responsible for mev-p binding. With that information PMK mutants could be screened for improvements in binding affinity. The crystallization of PMK was attempted, but our collaborators were unwilling to move forward

with that effort after failing to get any crystals on the first screen for two reasons. The first reason could be considered an initial design flaw in our protein expression. Because we had already been scooped in the publication of MK kinetics we wanted to get through the PMK experiments as quickly as possible, thus the C-terminal, six-histidine tag was not designed to be cleavable. This greatly reduced the amount of time necessary to express and purify PMK. However, it introduced a disordered region at the end of the protein that may have inhibited crystal formation. The second reason we had no control over, and that is the high ionic strength necessary for PMK to be soluble at high concentrations. The high salt concentrations were deemed too much of an impediment towards crystallography by our collaborators because of the high rate of false positives from salt crystals. Overcoming the first obstacle is a mere matter of cloning a cleavable his-tag. The second problem may be overcome by expressing PMK fused to another protein that will increase solubility or inhibit aggregation.

Acetyl-CoA C-acetyltransferase and Isopentenyl Diphosphate Isomerase

All of the *S. cerevisiae* enzymes from the mevalonate pathway have been characterized expect acetyl-CoA C-acetyltransferase (ACCA) and isopentenyl diphosphate isomerase (idi). The characterization of both MK and PMK revealed interesting information about their activities, so characterizing these last two enzymes could provide beneficial information about their activities. Although idi has previously been studied, the kinetic constants have not been determined, likely due to the difficulty involved with quantifying a double bond isomerization. Rather than a direct measurement idi activity, it may be possible to use IspA (the enzyme that converts IPP and DMAPP into FPP) in a coupled assay that measures FPP. Great care would need to be taken to ensure that idi is the rate limiting step; some necessary control experiments would be (1) to make sure the reaction rate does not change if the concentration of IspA is doubled and, (2) to make sure the reaction rate doubles when the concentration of idi is doubled. Because IspA acts only on IPP and DMAPP, there is no supporting substrate whose concentration can be altered to confirm that idi is the rate limiting step. ACCA should also be studied because the turnover number and K_M values reported in the BRENDA enzyme database for known ACCAs both span several orders of magnitude. Knowing where *S. cerevisiae* ACCA falls in that spectrum would help determine whether ACCA from another source should be incorporated into the engineered pathway.

Kinetic Modeling of the Mevalonate Pathway

Before undertaking any protein engineering efforts it might be informative to model the flux through the mevalonate pathway using the kinetic parameters of the enzymes. Given the feedback and substrate inhibition of MK, would altering any of the kinetic parameters of PMK theoretically increase the overall flux through the pathway? Would eliminating the substrate inhibition of MK theoretically increase the concentration of downstream metabolites, thus

worsening feedback inhibition? Is the simplest way to overcome feedback inhibition of MK to focus on ridding the system of prenyl phosphates as quickly as possible rather than engineer MK to have different properties? Since the pathway we are using is heterologous to *E. coli* it is unlikely that there are any native regulatory mechanisms, making a mathematical model of the lone pathway more promising for highlighting relevant engineering efforts.

Bibliography

Anderson MS, Muehlbacher M, Street IP, Proffitt J & Poulter CD (1989) Isopentenyl diphosphate:dimethylallyl diphosphate isomerase. An improved purification of the enzyme and isolation of the gene from Saccharomyces cerevisiae. *J Biol Chem* **264**: 19169-19175.

Andreassi JL, 2nd, Dabovic K & Leyh TS (2004) Streptococcus pneumoniae isoprenoid biosynthesis is downregulated by diphosphomevalonate: an antimicrobial target. *Biochemistry* **43**: 16461-16466.

Andreassi JL, 2nd, Bilder PW, Vetting MW, Roderick SL & Leyh TS (2007) Crystal structure of the Streptococcus pneumoniae mevalonate kinase in complex with diphosphomevalonate. *Protein Sci* **16**: 983-989.

Anthony JR, Anthony LC, Nowroozi F, Kwon G, Newman JD & Keasling JD (2009) Optimization of the mevalonate-based isoprenoid biosynthetic pathway in Escherichia coli for production of the anti-malarial drug precursor amorpha-4,11-diene. *Metab Eng* **11**: 13-19.

Bach TJ, Rogers DH & Rudney H (1986) Detergent-solubilization, purification, and characterization of membrane-bound 3-hydroxy-3-methylglutaryl-coenzyme A reductase from radish seedlings. *Eur J Biochem* **154**: 103-111.

Bennett GN & San K-Y (2009) Engineering *E. coli* Central Metabolism for Enhanced Primary Metabolite Production. (Lee SY, ed.), p. 351-376. Springer, Netherlands.

Berrios-Rivera SJ, San KY & Bennett GN (2002) The effect of NAPRTase overexpression on the total levels of NAD, the NADH/NAD+ ratio, and the distribution of metabolites in Escherichia coli. *Metab Eng* **4**: 238-247.

Berry A, Dodge TC, Pepsin M & Weyler W (2002) Application of metabolic engineering to improve both the production and use of biotech indigo. *J Ind Microbiol Biotechnol* **28**: 127-133.

Bischoff KM & Rodwell VW (1992) Biosynthesis and characterization of (S)-and (R)-3-hydroxy-3-methylglutaryl coenzyme A. *Biochem Med Metab Biol* **48**: 149-158.

Bloch K, Chaykin S, Phillips AH & De Waard A (1959) Mevalonic acid pyrophosphate and isopentenylpyrophosphate. *J Biol Chem* **234**: 2595-2604.

Bochar DA, Stauffacher CV & Rodwell VW (1999) Sequence comparisons reveal two classes of 3-hydroxy-3-methylglutaryl coenzyme A reductase. *Mol Genet Metab* **66**: 122-127.

Bokinsky G, Peralta-Yahya PP, George A*, et al.* (2011) Synthesis of three advanced biofuels from ionic liquid-pretreated switchgrass using engineered Escherichia coli. *Proc Natl Acad Sci U S A* **108**: 19949-19954.

Boucher Y, Huber H, L'Haridon S, Stetter KO & Doolittle WF (2001) Bacterial origin for the isoprenoid biosynthesis enzyme HMG-CoA reductase of the archaeal orders Thermoplasmatales and Archaeoglobales. *Mol Biol Evol* **18**: 1378-1388.

Chang MC, Eachus RA, Trieu W, Ro DK & Keasling JD (2007) Engineering Escherichia coli for production of functionalized terpenoids using plant P450s. *Nat Chem Biol* **3**: 274-277.

Chhabra S & Keasling J (2011) *Metabolic Design and Control for Production in Prokaryotes*. Elseveir, New York.

Chou HH & Keasling JD (2011) Host cells and methods for producing 3-methyl-2-buten-1-ol, 3-methyl-3-buten-1-ol, and 3-methyl-butan-1-ol. The Regents of the University of California.

Connolly DM & Winkler ME (1989) Genetic and physiological relationships among the miaA gene, 2-methylthio-N6-(delta 2-isopentenyl)-adenosine tRNA modification, and spontaneous mutagenesis in Escherichia coli K-12. *J Bacteriol* **171**: 3233-3246.

Dorsey JK & Porter JW (1968) The inhibition of mevalonic kinase by geranyl and farnesyl pyrophosphates. *J Biol Chem* **243**: 4667-4670.

Doun SS, Burgner JW, 2nd, Briggs SD & Rodwell VW (2005) Enterococcus faecalis phosphomevalonate kinase. *Protein Sci* **14**: 1134-1139.

Dueber JE, Wu GC, Malmirchegini GR*, et al.* (2009) Synthetic protein scaffolds provide modular control over metabolic flux. *Nat Biotechnol* **27**: 753-759.

Eyzaguirre J, Valdebenito D & Cardemil E (2006) Pig liver phosphomevalonate kinase: kinetic mechanism. *Arch Biochem Biophys* **454**: 189-196.

Fortman JL, Chhabra S, Mukhopadhyay A, Chou H, Lee TS, Steen E & Keasling JD (2008) Biofuel alternatives to ethanol: pumping the microbial well. *Trends Biotechnol* **26**: 375-381.

Fu Z, Voynova NE, Herdendorf TJ, Miziorko HM & Kim JJ (2008) Biochemical and structural basis for feedback inhibition of mevalonate kinase and isoprenoid metabolism. *Biochemistry* **47**: 3715-3724.

Glick BR (1995) Metabolic load and heterologous gene expression. *Biotechnol Adv* **13**: 247-261.

Harada H & Misawa N (2009) Novel approaches and achievements in biosynthesis of functional isoprenoids in Escherichia coli. *Appl Microbiol Biotechnol* **84**: 1021-1031.

Hedl M, Tabernero L, Stauffacher CV & Rodwell VW (2004) Class II 3-hydroxy-3-methylglutaryl coenzyme A reductases. *J Bacteriol* **186**: 1927-1932.

Heuser F, Schroer K, Luetz S, Bringer-Meyer S & Sahm H (2007) Enhancement of the NAD(P)(H) pool in Escherichia coli for biotransformation. *Engineering in Life Sciences* **7**: 343-353.

Hinson DD, Chambliss KL, Toth MJ, Tanaka RD & Gibson KM (1997) Post-translational regulation of mevalonate kinase by intermediates of the cholesterol and nonsterol isoprene biosynthetic pathways. *J Lipid Res* **38**: 2216-2223.

Hunter GA & Ferreira GC (2010) Identification and characterization of an inhibitory metal ion-binding site in ferrochelatase. *J Biol Chem* **285**: 41836-41842.

Istvan ES (2001) Bacterial and mammalian HMG-CoA reductases: related enzymes with distinct architectures. *Curr Opin Struct Biol* **11**: 746-751.

Kim DY, Stauffacher CV & Rodwell VW (2000) Dual coenzyme specificity of Archaeoglobus fulgidus HMG-CoA reductase. *Protein Sci* **9**: 1226-1234.

Krepkiy D & Miziorko HM (2004) Identification of active site residues in mevalonate diphosphate decarboxylase: implications for a family of phosphotransferases. *Protein Sci* **13**: 1875-1881.

Kuzuyama T (2002) Mevalonate and nonmevalonate pathways for the biosynthesis of isoprene units. *Biosci Biotechnol Biochem* **66**: 1619-1627.

Kuzuyama T & Seto H (2012) Two distinct pathways for essential metabolic precursors for isoprenoid biosynthesis. *Proc Jpn Acad Ser B Phys Biol Sci* **88**: 41-52.

Lawrence CM, Chi YI, Rodwell VW & Stauffacher CV (1995) Crystallization of HMG-CoA reductase from Pseudomonas mevalonii. *Acta Crystallogr D Biol Crystallogr* **51**: 386-389.

Lee SK, Chou H, Ham TS, Lee TS & Keasling JD (2008) Metabolic engineering of microorganisms for biofuels production: from bugs to synthetic biology to fuels. *Curr Opin Biotechnol* **19**: 556-563.

Ma SM, Garcia DE, Redding-Johanson AM*, et al.* (2011) Optimization of a heterologous mevalonate pathway through the use of variant HMG-CoA reductases. *Metab Eng* **13**: 588-597.

Martin VJ, Pitera DJ, Withers ST, Newman JD & Keasling JD (2003) Engineering a mevalonate pathway in Escherichia coli for production of terpenoids. *Nat Biotechnol* **21**: 796-802.

Middleton B (1972) KINETIC MECHANISM OF 3-HYDROXY-3-METHYLGLUTARYL-COENZYME-A SYNTHASE FROM BAKERS-YEAST. *Biochemical Journal* **126**: 35-47.

Peralta-Yahya PP, Ouellet M, Chan R, Mukhopadhyay A, Keasling JD & Lee TS (2011) Identification and microbial production of a terpene-based advanced biofuel. *Nat Commun* **2**: 483.

Pfleger BF, Pitera DJ, Smolke CD & Keasling JD (2006) Combinatorial engineering of intergenic regions in operons tunes expression of multiple genes. *Nat Biotechnol* **24**: 1027-1032.

Pilloff D, Dabovic K, Romanowski MJ, Bonanno JB, Doherty M, Burley SK & Leyh TS (2003) The kinetic mechanism of phosphomevalonate kinase. *J Biol Chem* **278**: 4510-4515.

Pitera DJ, Paddon CJ, Newman JD & Keasling JD (2007) Balancing a heterologous mevalonate pathway for improved isoprenoid production in Escherichia coli. *Metab Eng* **9**: 193-207.

Potter D, Wojnar JM, Narasimhan C & Miziorko HM (1997) Identification and functional characterization of an active-site lysine in mevalonate kinase. *J Biol Chem* **272**: 5741-5746.

Primak YA, Du M, Miller MC, Wells DH, Nielsen AT, Weyler W & Beck ZQ (2011) Characterization of a feedback-resistant mevalonate kinase from the archaeon Methanosarcina mazei. *Appl Environ Microbiol* **77**: 7772-7778.

Redding-Johanson AM, Batth TS, Chan R*, et al.* (2011) Targeted proteomics for metabolic pathway optimization: application to terpene production. *Metab Eng* **13**: 194-203.

Ro DK, Paradise EM, Ouellet M*, et al.* (2006) Production of the antimalarial drug precursor artemisinic acid in engineered yeast. *Nature* **440**: 940-943.

Rodwell VW, Beach MJ, Bischoff KM*, et al.* (2000) 3-Hydroxy-3-methylglutaryl-CoA reductase. *Methods Enzymol* **324**: 259-280.

Salis HM (2011) THE RIBOSOME BINDING SITE CALCULATOR. *Synthetic Biology, Pt B: Computer Aided Design and DNA Assembly,* Vol. 498 (Voigt C, ed.), p. 19-42.

San KY, Bennett GN, Berrios-Rivera SJ*, et al.* (2002) Metabolic engineering through cofactor manipulation and its effects on metabolic flux redistribution in Escherichia coli. *Metab Eng* **4**: 182-192.

Schneider DA & Gourse RL (2004) Relationship between growth rate and ATP concentration in Escherichia coli: a bioassay for available cellular ATP. *J Biol Chem* **279**: 8262-8268.

Sherban DG, Kennelly PJ, Brandt KG & Rodwell VW (1985) Rat liver 3-hydroxy-3-methylglutaryl-CoA reductase. Catalysis of the reverse reaction and two half-reactions. *J Biol Chem* **260**: 12579-12585.

Singh P, Batth TS, Juminaga D, Dahl RH, Keasling JD, Adams PD & Petzold CJ (2012) Application of targeted proteomics to metabolically engineered Escherichia coli. *Proteomics* **12**: 1289-1299.

Song L (1994) Yeast Farnesyl-Diphosphate Synthase: Site-Directed Mutagenesis of Residues in Highly Conserved Prenyltransferase Domains I and II. *Proceedings of the National Academy of Sciences* **91**: 3044-3048.

Theivagt AE, Amanti EN, Beresford NJ, Tabernero L & Friesen JA (2006) Characterization of an HMG-CoA reductase from Listeria monocytogenes that exhibits dual coenzyme specificity. *Biochemistry* **45**: 14397-14406.

von Ballmoos C, Wiedenmann A & Dimroth P (2009) Essentials for ATP Synthesis by F1F0 ATP Synthases. *Annual Review of Biochemistry* **78**: 649-672.

Voynova NE, Rios SE & Miziorko HM (2004) Staphylococcus aureus mevalonate kinase: isolation and characterization of an enzyme of the isoprenoid biosynthetic pathway. *J Bacteriol* **186**: 61-67.

Wilding EI, Brown JR, Bryant AP*, et al.* (2000) Identification, evolution, and essentiality of the mevalonate pathway for isopentenyl diphosphate biosynthesis in gram-positive cocci. *J Bacteriol* **182**: 4319-4327.

Zhang F, Rodriguez S & Keasling JD (2011) Metabolic engineering of microbial pathways for advanced biofuels production. *Curr Opin Biotechnol* **22**: 775-783.

Zhang W, Li Y & Tang Y (2008) Engineered biosynthesis of bacterial aromatic polyketides in Escherichia coli. *Proc Natl Acad Sci U S A* **105**: 20683-20688.

Zhu MM, Lawman PD & Cameron DC (2002) Improving 1,3-propanediol production from glycerol in a metabolically engineered Escherichia coli by reducing accumulation of sn-glycerol-3-phosphate. *Biotechnol Prog* **18**: 694-699.

Appendix

Table 2. The *E. coli* codon-optimized sequence for mevalonate kinase from *S. cerevisiae*.

ATGAGCCTG CCATTCCTG ACGAGCGCC CCTGGTAAA GTAATCATT TTTGGCGAG
CATTCTGCG GTTTACAAT AAGCCGGCA GTGGCAGCG AGCGTGAGC GCCCTGCGT
ACCTATCTG CTGATCTCT GAAAGCAGC GCTCCGGAT ACCATTGAA CTGGACTTC
CCGGACATT AGCTTTAAC CACAAATGG AGCATCAAT GATTTCAAT GCCATTACC
GAGGACCAA GTTAACAGC CAGAAGCTG GCAAAGGCG CAGCAAGCG ACCGATGGT
CTGAGCCAG GAGCTGGTA AGCCTGCTG GACCCGCTG CTGGCGCAG CTGTCCGAA
AGCTTCCAT TACCATGCT GCCTTTTGC TTCCTGTAC ATGTTTGTT TGTCTGTGT
CCGCACGCA AAGAACATC AAGTTTTCG CTGAAGAGC ACCTTGCCA ATTGGCGCA
GGTCTGGGC AGCAGCGCT TCGATTAGC GTCAGCCTG GCGCTGGCA ATGGCCTAC
TTGGGCGGT CTGATCGGT TCCAACGAT CTGGAGAAA CTGTCCGAA AACGACAAA
CACATCGTG AATCAATGG GCTTTCATC GGTGAAAAG TGCATTCAC GGCACCCCG
AGCGGCATT GATAACGCG GTTGCGACC TATGGTAAC GCTCTGCTG TTTGAAAAG
GACAGCCAC AACGGTACG ATCAATACG AATAACTTT AAGTTCCTG GACGATTTC
CCTGCCATC CCGATGATC CTGACCTAT ACTCGTATT CCGCGTAGC ACCAAGGAC
CTGGTTGCT CGCGTCCGC GTCCTGGTC ACCGAGAAA TTCCCGGAG GTTATGAAA
CCGATTCTG GACGCGATG GGCGAGTGC GCGTTGCAG GGTTTGGAG ATTATGACG
AAACTGAGC AAATGCAAA GGCACCGAT GACGAGGCG GTGGAGACG AACAATGAA
CTGTATGAG CAACTGCTG GAACTGATC CGCATCAAT CACGGTCTG CTGGTTAGC
ATTGGTGTG AGCCACCCG GGTCTGGAG CTGATCAAG AACCTGAGC GACGACCTG
CGTATCGGC AGCACCAAG CTGACCGGT GCGGGTGGT GGTGGTTGC AGCCTGACC
TTGCTGCGT CGTGATATT ACCCAAGAA CAGATCGAT TCCTTTAAG AAGAAACTG
CAAGATGAT TTCTCTTAC GAAACGTTC GAGACGGAT TTGGGCGGT ACGGGTTGT
TGTCTGCTG TCCGCGAAA AATCTGAAT AAAGACCTG AAGATCAAG TCCCTGGTC
TTTCAGCTG TTCGAAAAC AAAACCACG ACCAAGCAG CAGATTGAC GATTTGCTG
CTGCCGGGT AATACCAAC TTGCCGTGG ACCTCCTAA

Table 3. The *E. coli* codon-optimized sequence for phosphomevalonate kinase from *S. cerevisiae*.

ATGAGCGAA TTACGTGCA TTCAGCGCG CCAGGTAAG GCACTGCTG GCCGGTGGC
TACCTGGTG TTAGACACC AAGTACGAG GCGTTCGTC GTCGGCTTA TCTGCCCGT
ATGCATGCA GTTGCCCAC CCGTATGGT AGCCTGCAG GGCTCTGAC AAGTTCGAA
GTGCGTGTG AAGAGCAAG CAGTTCAAG GACGGCGAG TGGCTGTAC CACATTAGC
CCAAAGAGC GGCTTCATC CCGGTTAGC ATTGGTGGC AGCAAGAAC CCATTTATC
GAGAAGGTC ATTGCCAAC GTCTTCAGC TACTTCAAG CCGAATATG GACGATTAC
TGCAACCGC AACCTGTTC GTCATCGAC ATTTTCAGC GACGACGCG TACCACAGC
CAAGAGGAC TCTGTTACG GAGCATCGT GGTAACCGC CGCCTGAGC TTCCACAGC
CATCGCATT GAGGAGGTG CCGAAGACG GGTCTGGGT TCTAGCGCC GGTTTAGTT
ACCGTCTTA ACGACGGCG TTAGCGAGC TTCTTCGTG AGCGACCTG GAGAACAAC
GTGGACAAG TACCGCGAA GTGATTCAT AACCTGGCG CAGGTGGCA CATTGTCAG
GCCCAAGGT AAGATTGGC TCTGGTTTT GATGTGGCA GCGGCCGCC TATGGCTCT
ATCCGCTAT CGCCGCTTT CCGCCGGCC CTGATCAGC AATCTGCCG GACATCGGC
TCTGCGACG TATGGTAGC AAACTGGCG CATCTGGTG GACGAGGAG GACTGGAAC
ATCACCATT AAGTCTAAT CACCTGCCG AGCGGCTTA ACGTTATGG ATGGGCGAT
ATCAAGAAC GGCAGCGAA ACGGTTAAG CTGGTGCAG AAAGTGAAA AACTGGTAC
GACAGCCAC ATGCCGGAA AGCCTGAAG ATTTACACG GAGCTGGAC CACGCCAAT
AGCCGTTTC ATGGATGGT CTGAGCAAG CTGGACCGC CTGCACGAA ACCCACGAC
GACTACAGC GACCAGATC TTCGAGAGC CTGGAGCGC AATGACTGC ACCTGCCAG
AAGTACCCG GAGATCACG GAGGTCCGC GATGCCGTG GCAACGATT CGCCGTAGC
TTCCGCAAA ATTACGAAG GAGAGCGGC GCGGATATC GAACCACCG GTCCAGACG
TCTCTGCTG GACGACTGT CAAACCTTA AAGGGCGTG TTAACGTGC CTGATTCCG
GGCGCGGGT GGTTACGAC GCCATTGCC GTCATCACG AAACAGGAC GTCGATCTG
CGCGCACAA ACGGCCAAC GACAAACGT TTCAGCAAA GTCCAATGG CTGGATGTT
ACGCAGGCC GACTGGGGT GTTCGCAAG GAGAAGGAC CCGGAAACG TATCTGGAT
AAGTGA